Nanoscale Measurement Methods for Novel Material Characterization

J. Alexander Liddle, Gila E. Stein,[1] Joseph A. Stroscio, Nikolai B. Zhitenev,

P. N. First,[2] and W. A. de Heer[2]

CNST Center for Nanoscale Science & Technology

[1]Department of Chemical & Biomolecular Engineering, University of Houston
[2]School of Physics, Georgia Institute of Technology

NIST National Institute of Standards and Technology • U.S. Department of Commerce

Diblock Copolymers for Advanced Patterning

- Pitch and LER limit circuit density and device uniformity
- Diblock copolymers might help
- Significant optimization needed
- How do we measure their behavior?

Diblock Copolymers

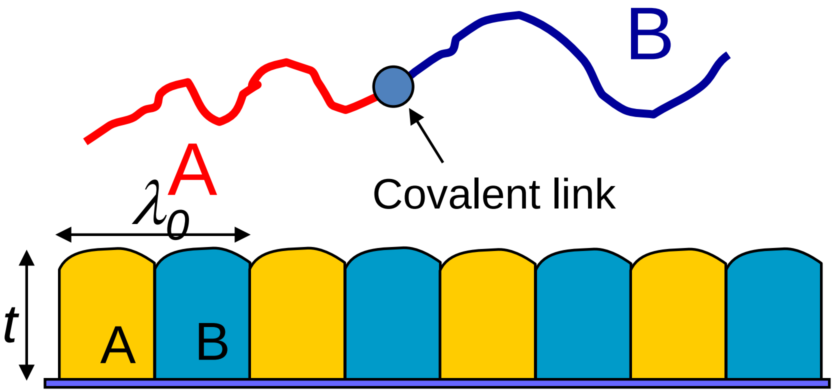

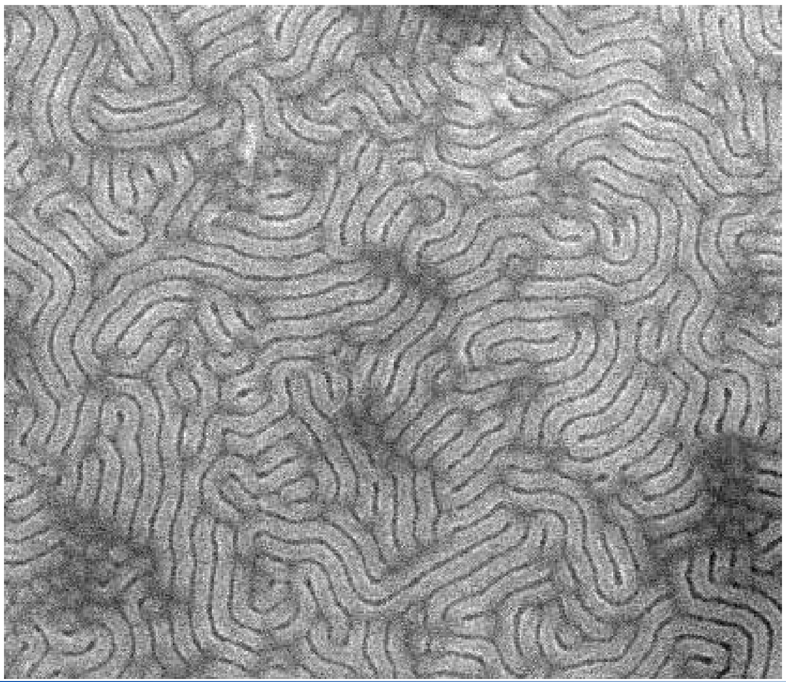

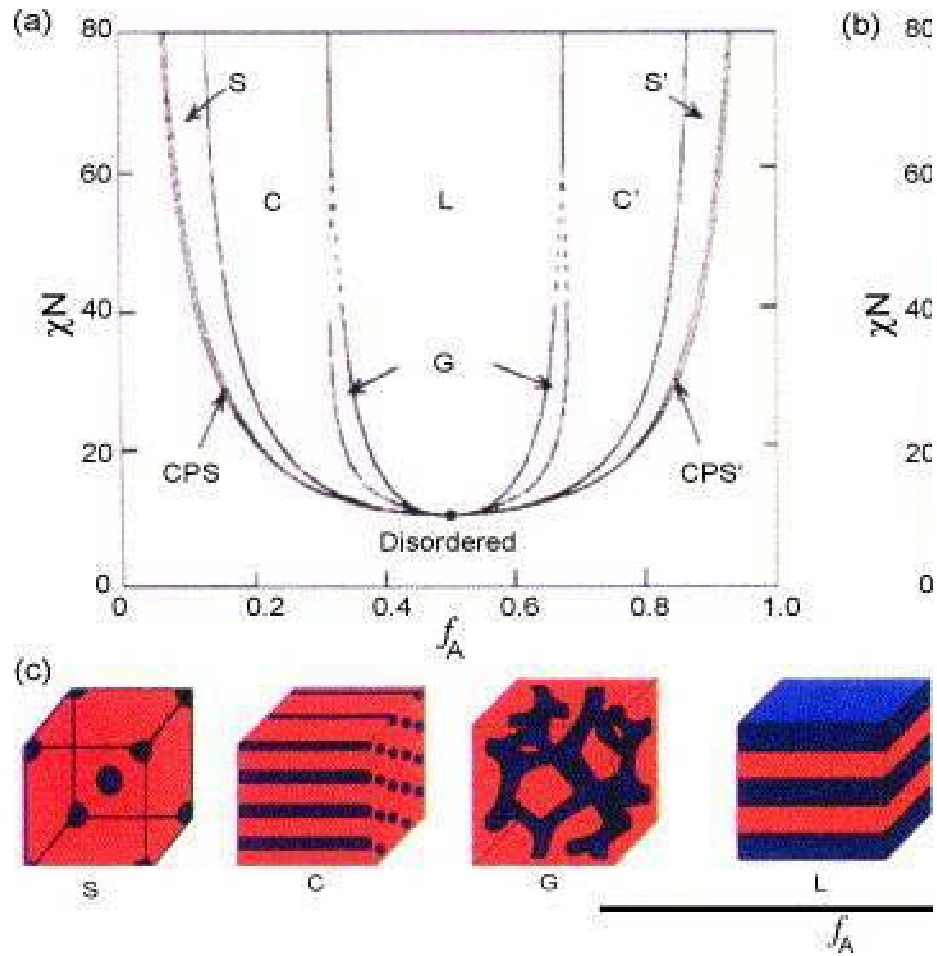

From *"Block Copolymers - Designer Soft Materials"*, F.S. Bates and G.H. Frederickson, *Physics Today*, **Feb.** 32 (1999)

Diblock Epitaxy

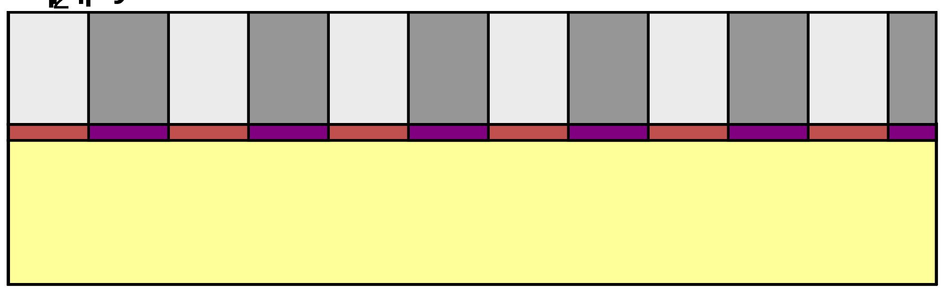

Diblock Epitaxy

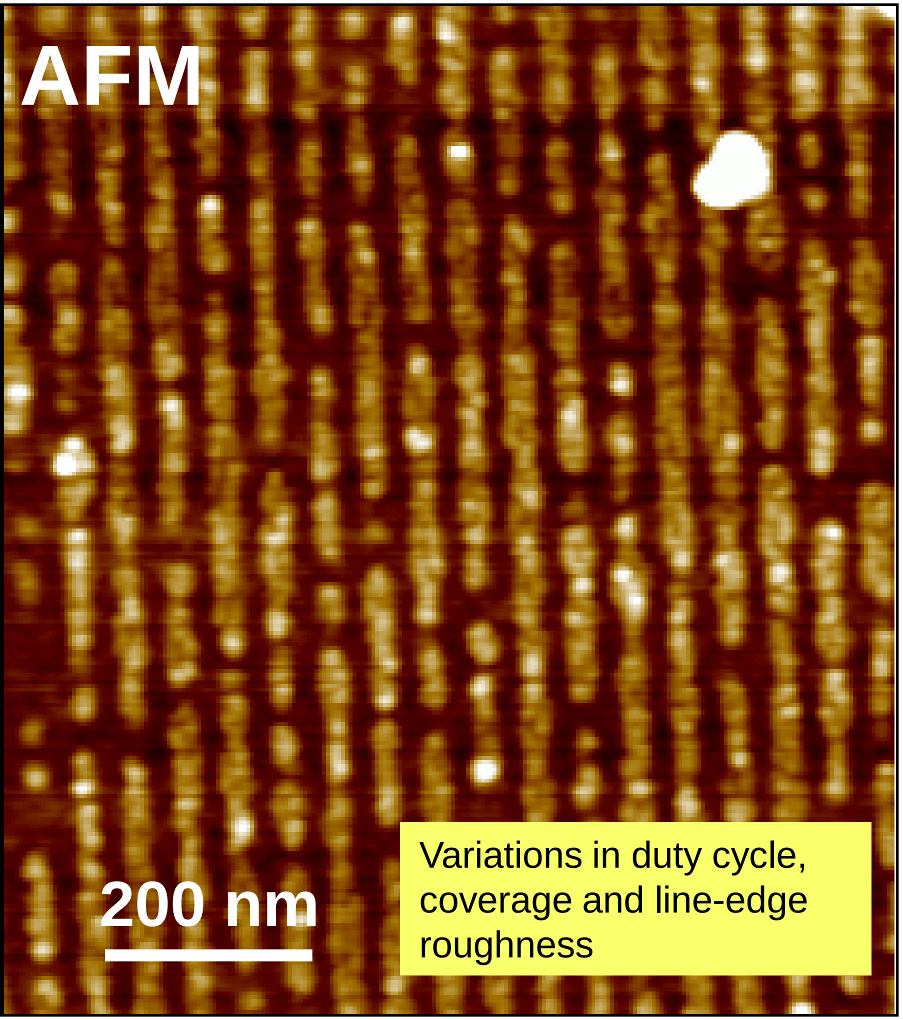

Variations in duty cycle, coverage and line-edge roughness

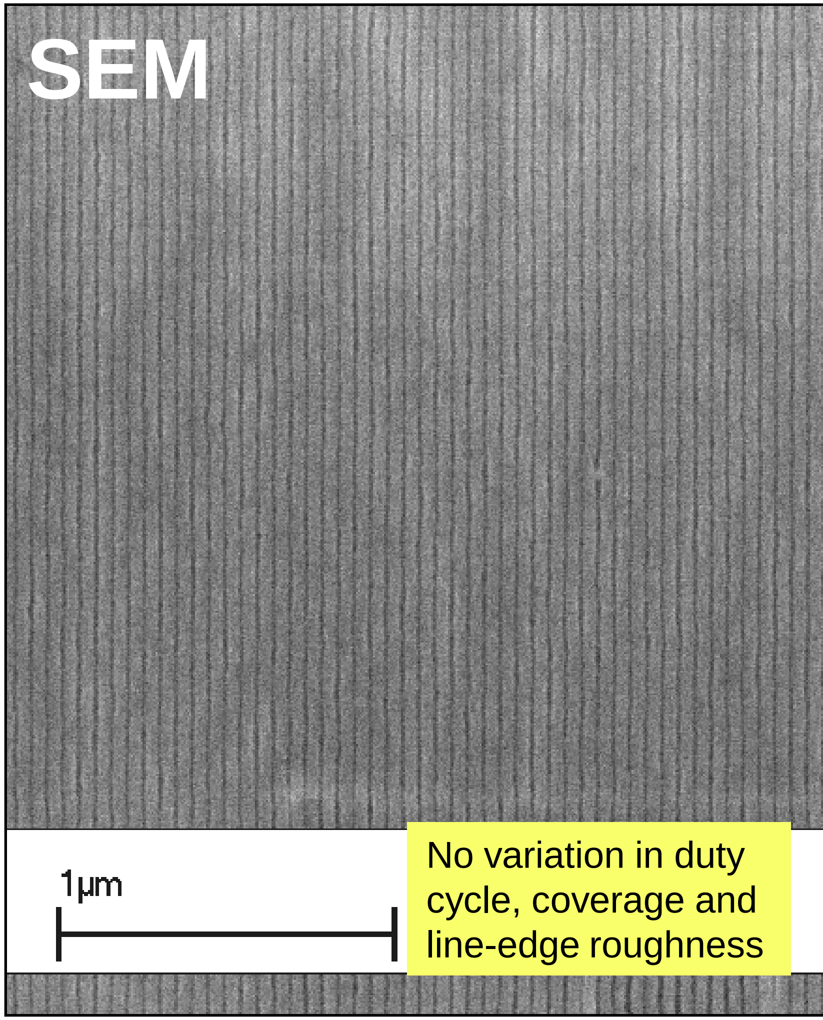

No variation in duty cycle, coverage and line-edge roughness

Sub-Lithographic Patterns

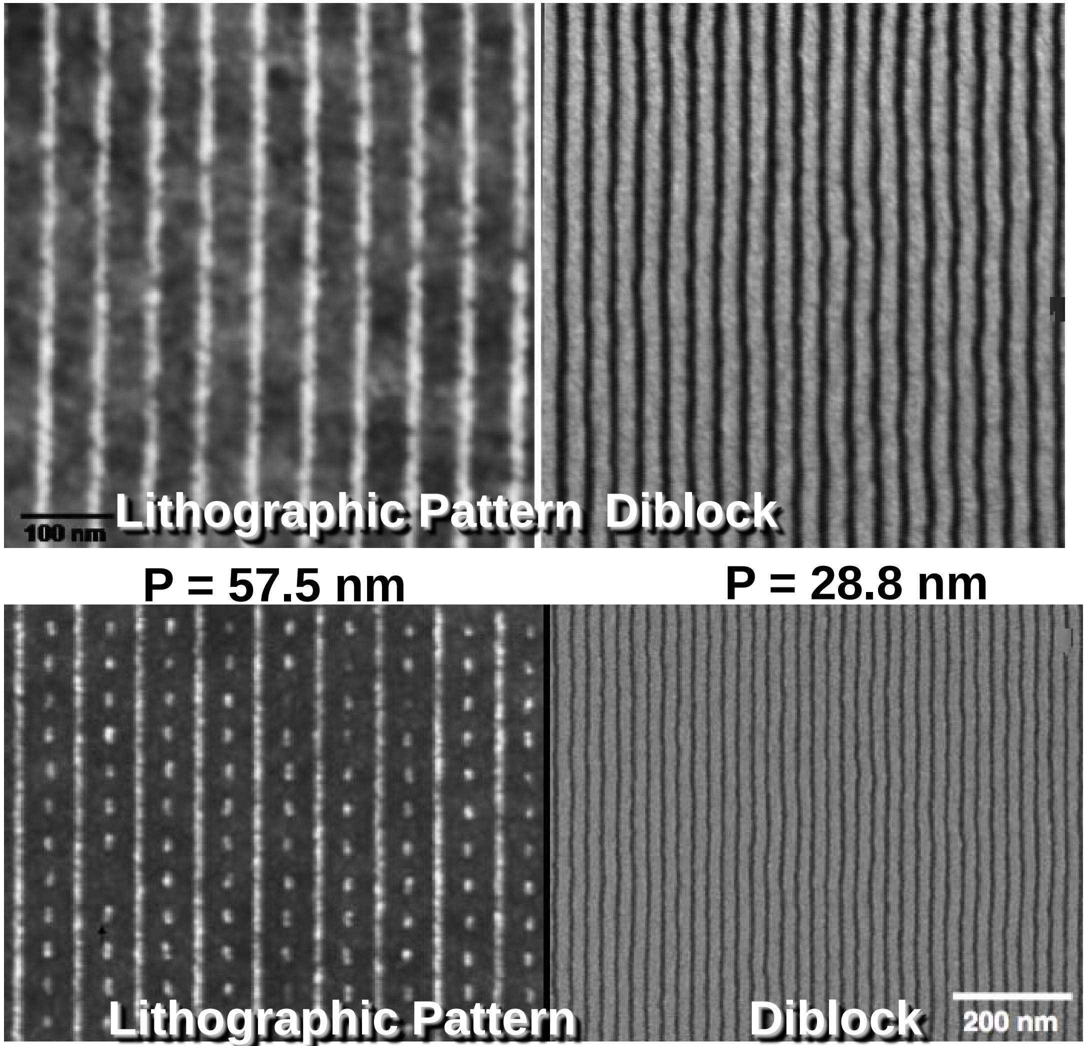

Dense Self-Assembly on Sparse Chemical Patterns: Rectifying and Multiplying Lithographic Patterns Using Block Copolymers, Joy Y. Cheng, Charles T. Rettner, Daniel P. Sanders, Ho-Cheol Kim, and William D. Hinsberg, Advanced Materials, (2008) - IBM

LER from SEM

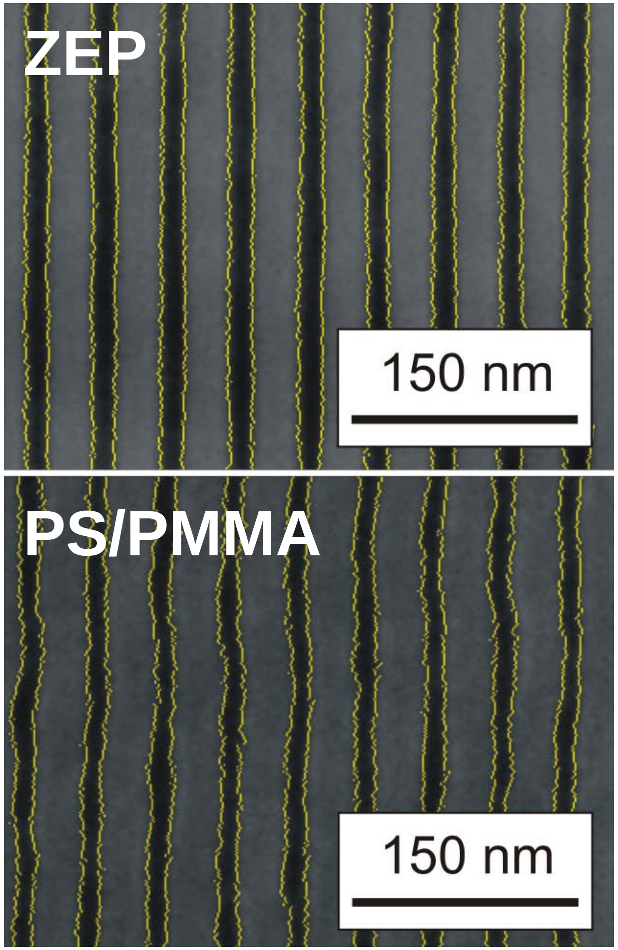
ZEP
150 nm
PS/PMMA
150 nm

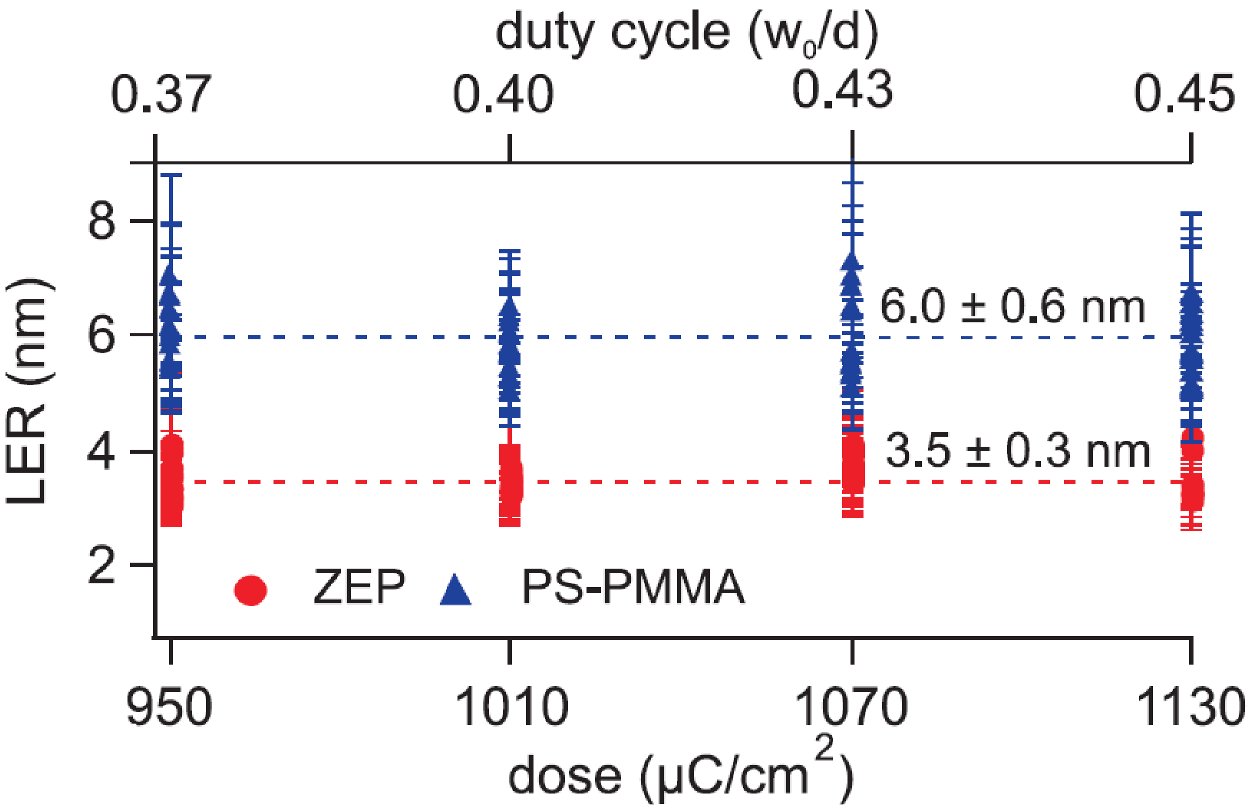
duty cycle (w_0/d)
0.37
0.40
0.43
0.45
LER (nm)
8
6
4
2
6.0 ± 0.6 nm
3.5 ± 0.3 nm
ZEP
PS-PMMA
950
1010
1070
1130
dose (μC/cm^2)

Resonant X-ray Scattering

Are interfaces sharp, chemically diffuse or rough?

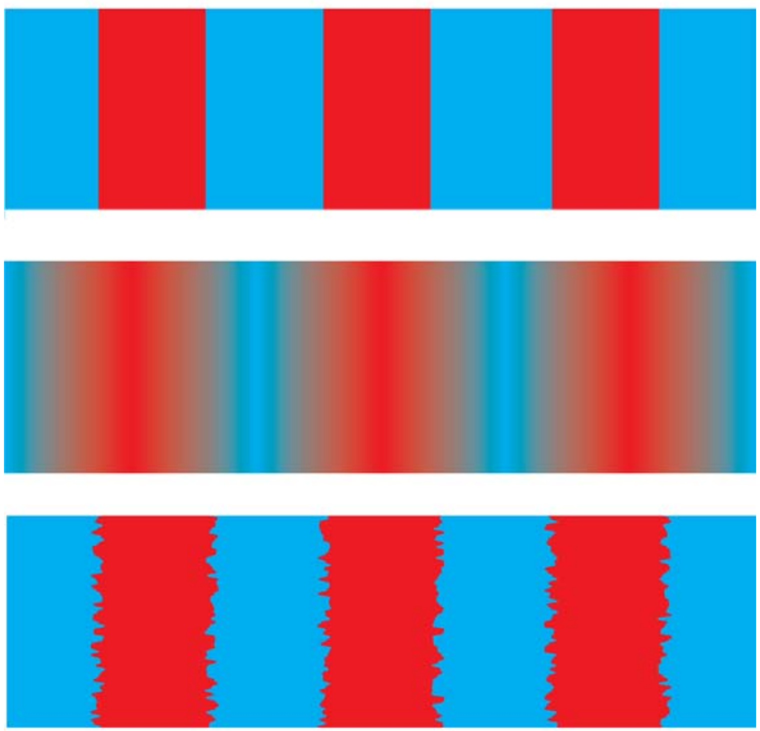

Virgili et al. Macromolecules (2007)

- X-ray scattering can measure interfacial width or roughness to sub-0.5 nm accuracy.
- Different chemistries have distinct resonances
- Resonant scattering enhances contrast from different chemical domains
- C=C π^* 285 eV, C=O π^* 288 eV, C-O σ^* 293 eV

PS PMMA ZEP

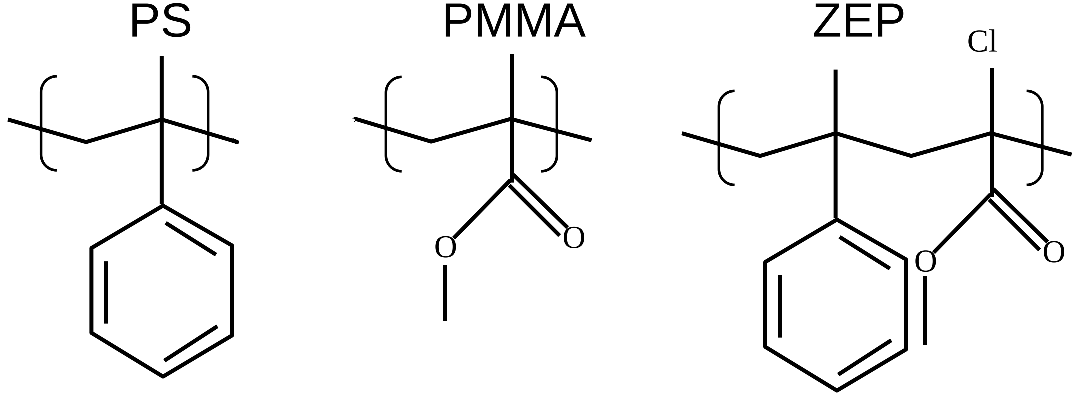

Random Diblock Diffraction

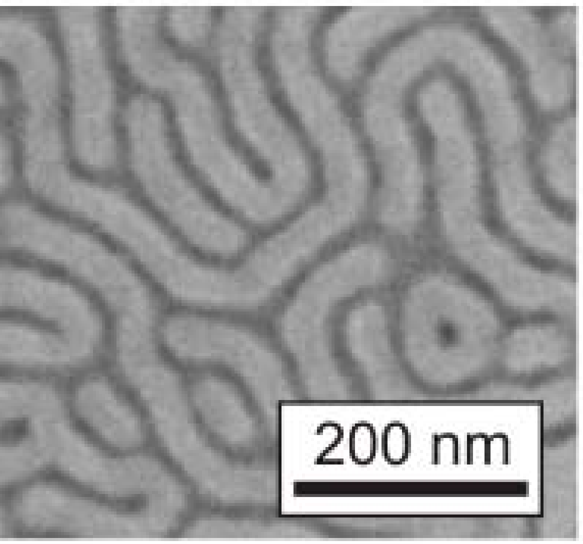

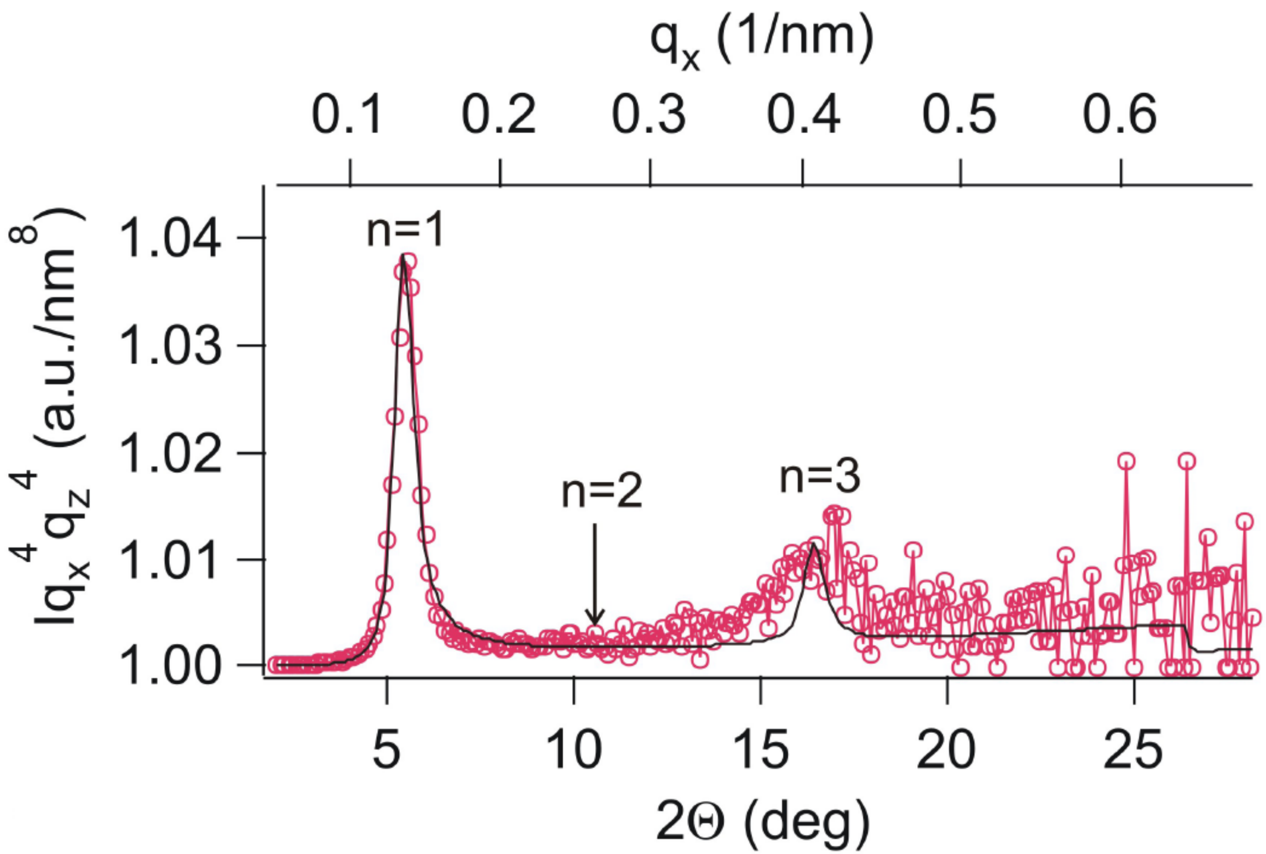

Epitaxial Diblock Diffraction

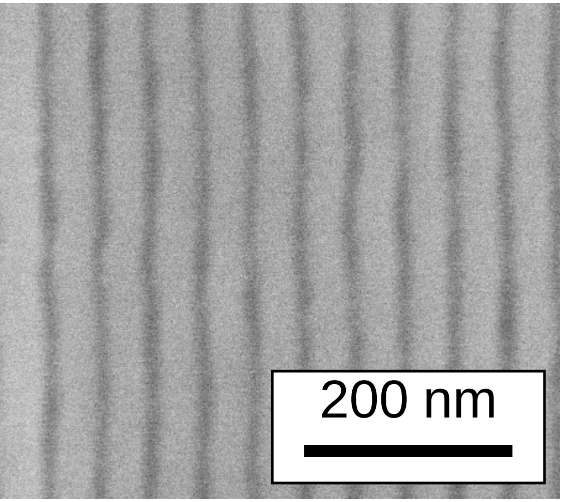

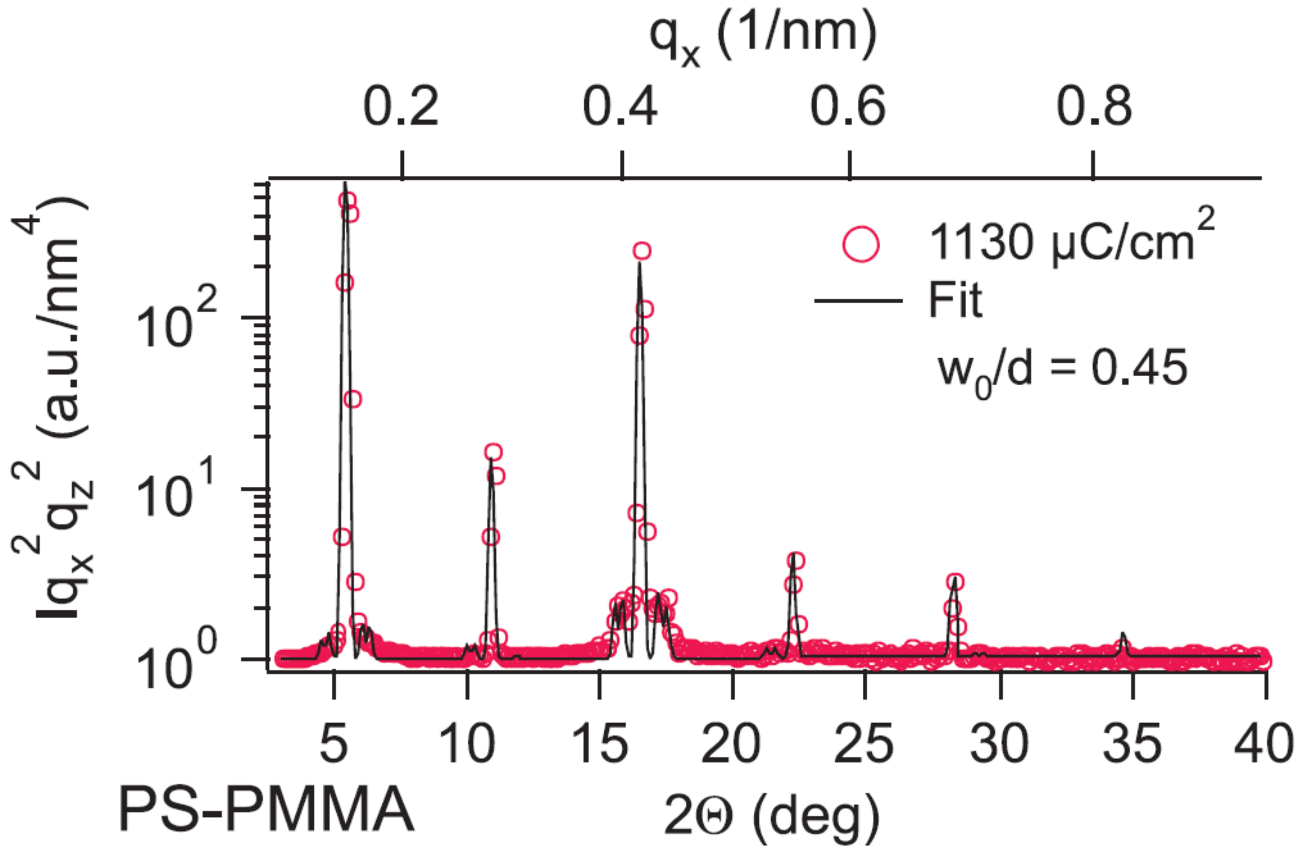

PS-PMMA

Interface Width from XRD

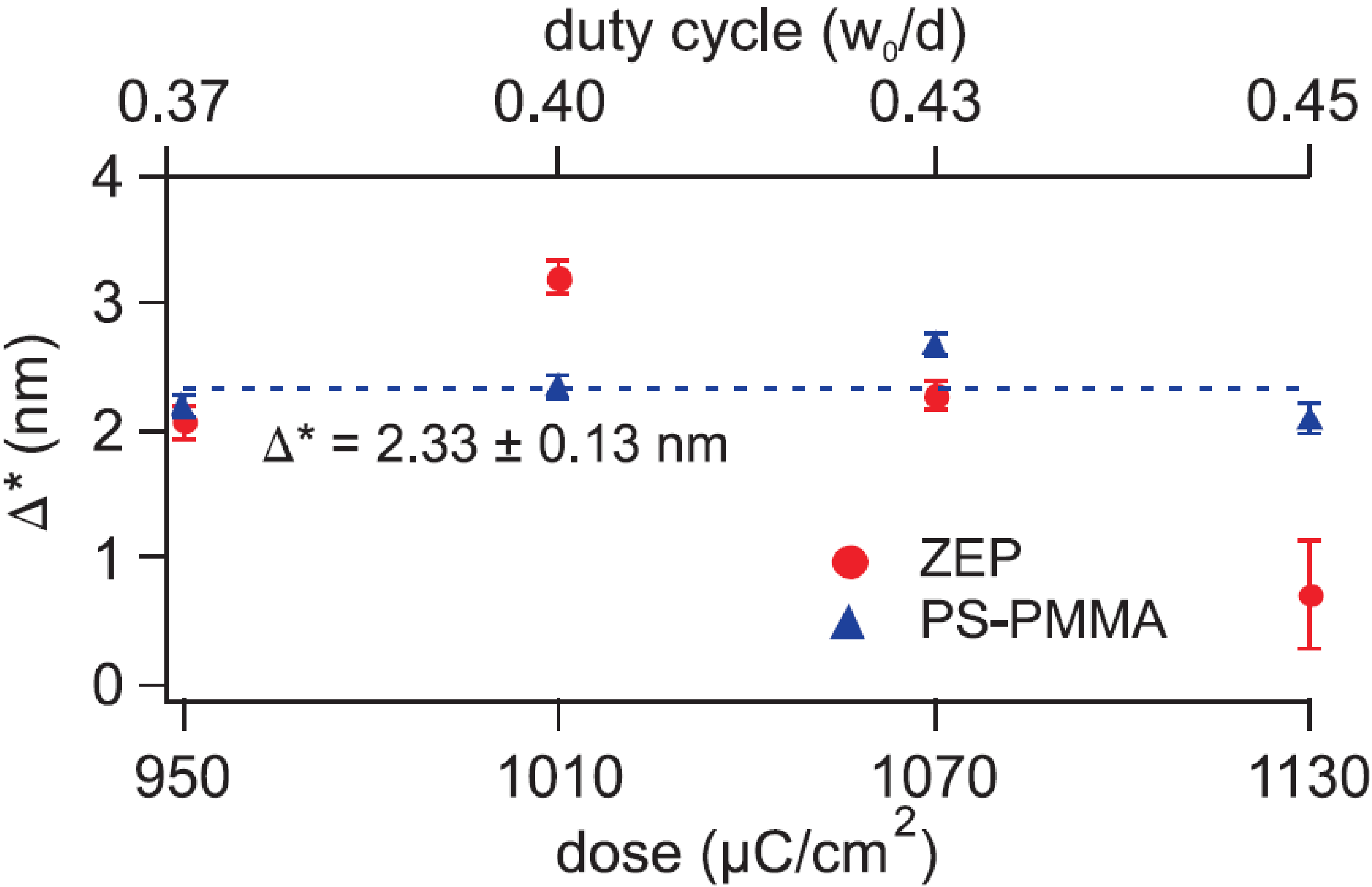

Summary

- X-ray diffraction samples large areas
- Resonant scattering provides chemical contrast – diblocks, latent images, etc.
- Patterned nanostructure arrays yield lots of information
- Analysis relies on model

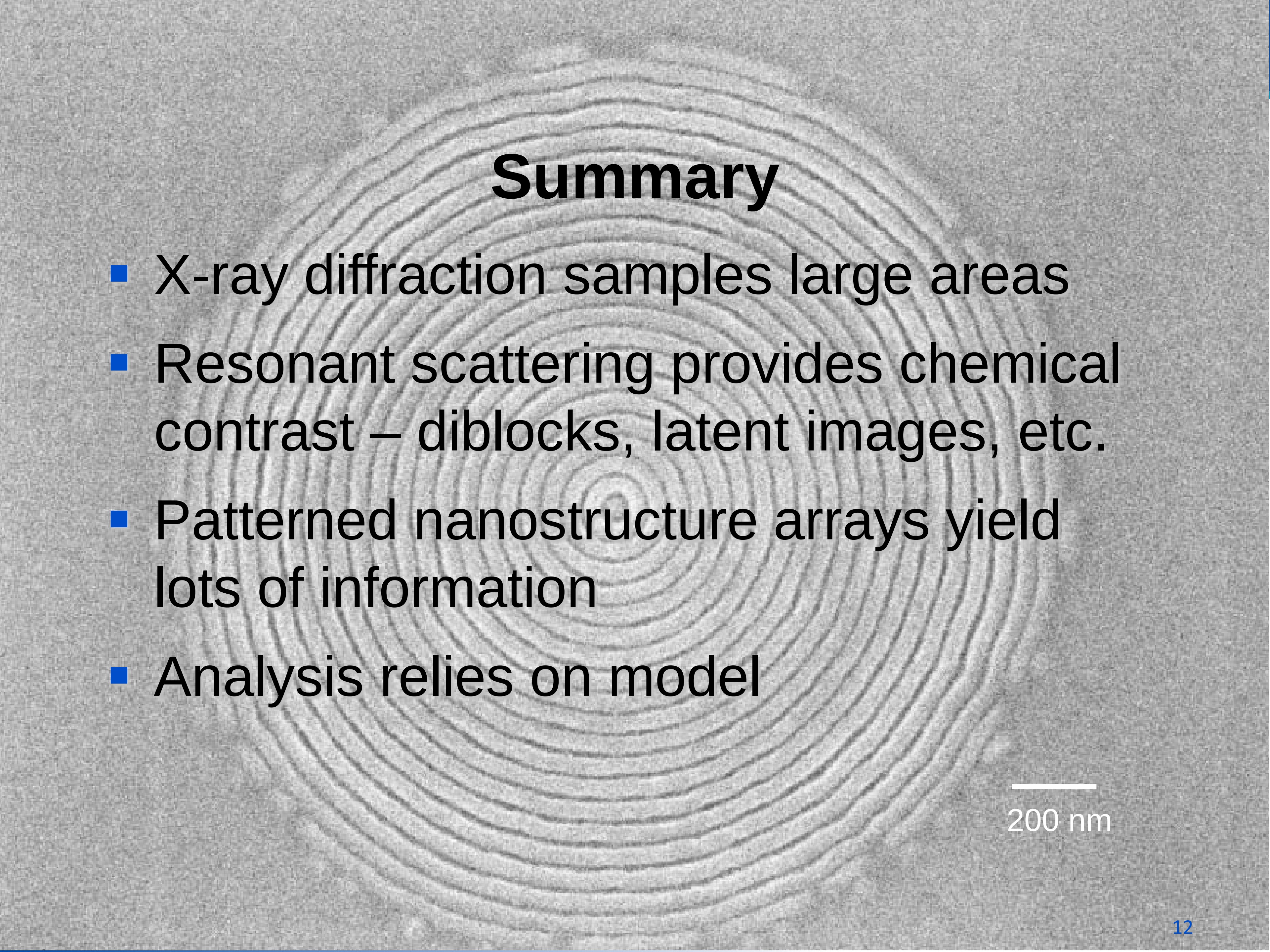

Solar Cells for Large-area Electronics

- Most work on material development, or device efficiency by trial and error
- Correlation of film morphology and charge transport not known
- Novel combined electrical and optical techniques needed

Organic PV Cell

- Donor and acceptor separate charge carriers
- Efficiency low in layered systems because of short exciton diffusion length
- Nanostructured blends reduce required length

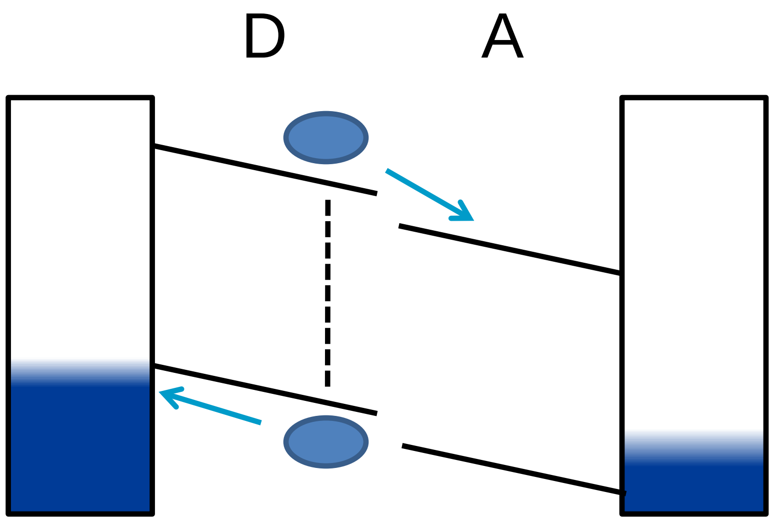

Blended Organic Solar Cells

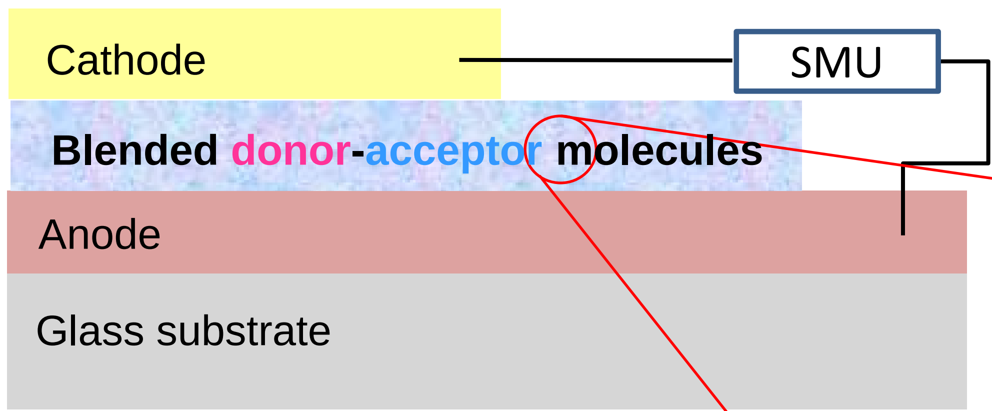

Bulk heterojunction

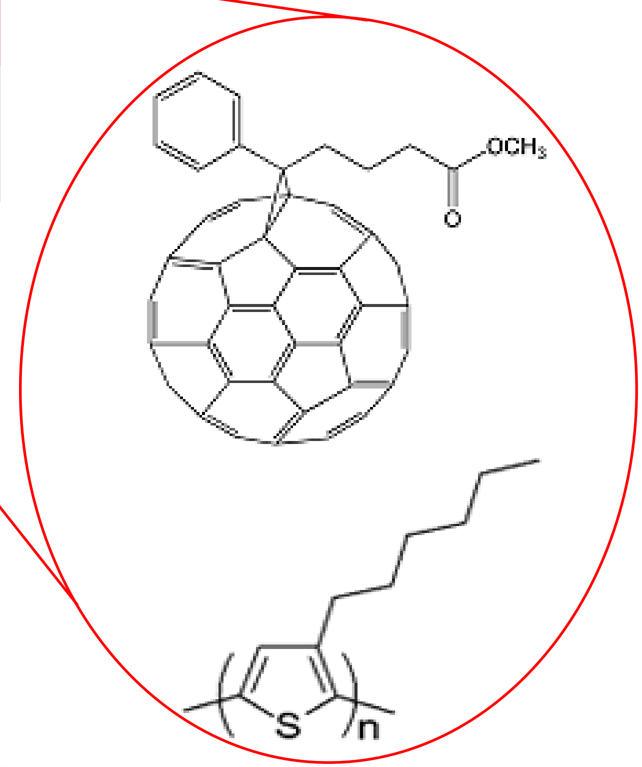

1:1 blend of Poly(3-hexylthiophene) (P3HT) to [6,6]-phenyl-C_{61}-butyric acid methyl ester (PCBM).

SPM Photocurrent Measurements

Photoresponse current measured with a conductive tip in contact mode while simultaneously mapping the surface topography.

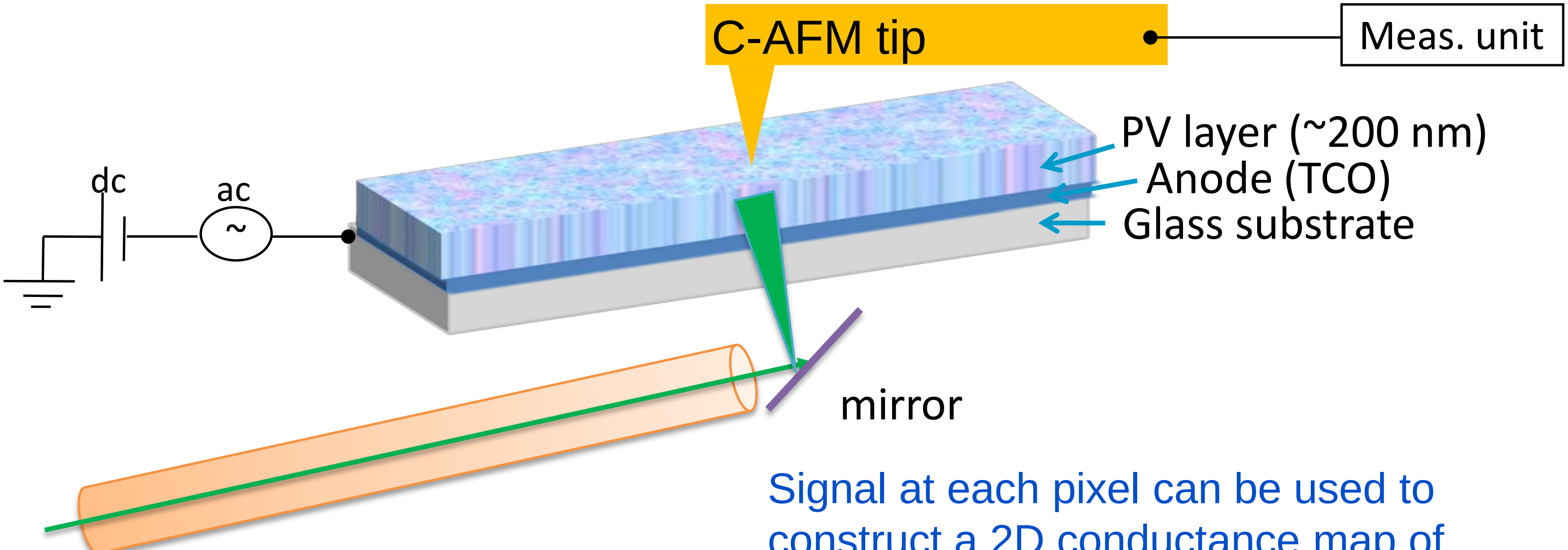

532 nm laser focused into fiber optic cable

Signal at each pixel can be used to construct a 2D conductance map of the surface.

C-AFM Measurement

Coffey et. al. (NanoLett 2007) – 1st photoconductive AFM of nanoscale morphology vs locally detected photocurrent.

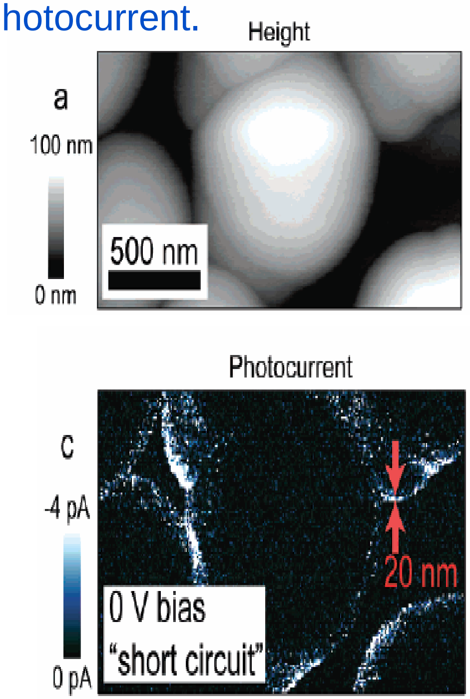

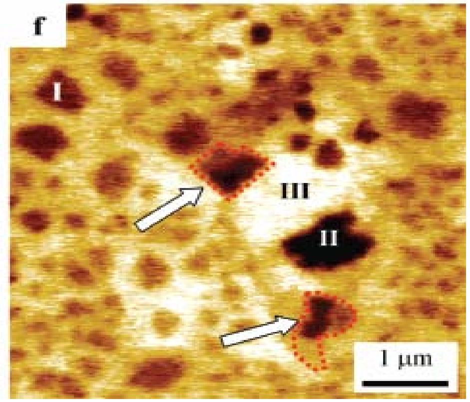

A. Liscio et. al, (JACS 2008) - Correlation of surface potential with film morphology: Scanning Probe Force microscope.

O. Douheret et. al. (Prog. Photovolt 2007) - C-AFM of blended OPV materials: morphology vs charge transport .

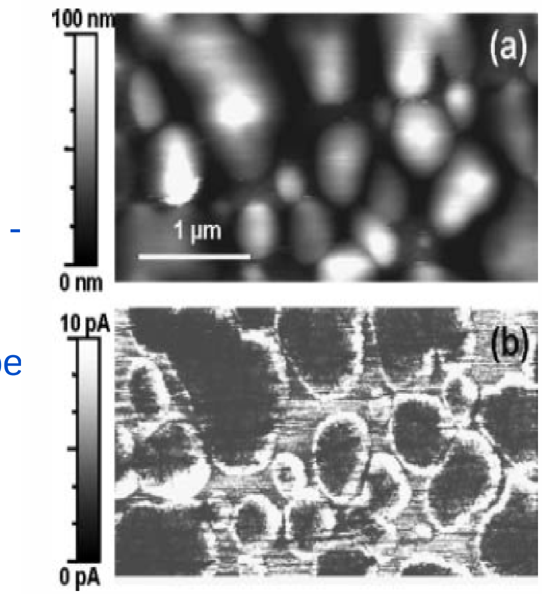

- Most of these lack detailed quantitative analysis and a broad understanding. However, they have opened the door for a plethora of new problems to investigate!

Macroscopic Measurements

- Absorption and spectral response measure optical/electro-optical quality of PV films/devices.

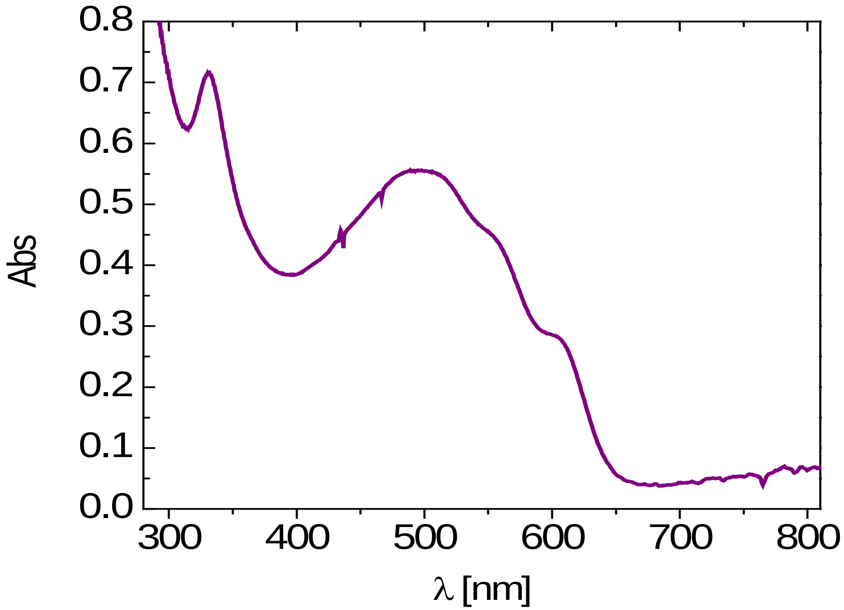

UV-Vis for solution-processed P3HT:PCBM spun cast on glass. 500 nm: p-type polymer absorption (electron donor) 325 nm: n-type PCBM molecules.

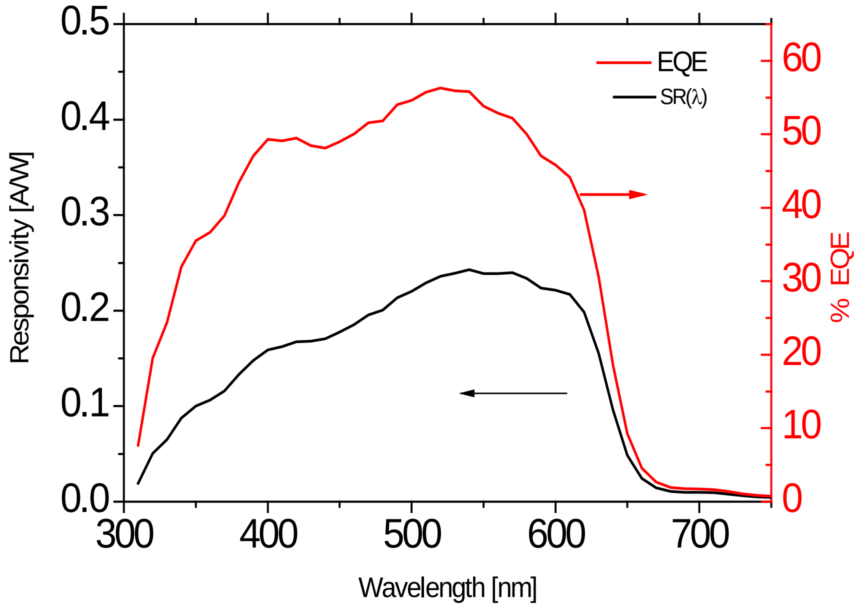

Responsivity and (EQE) of OPV device with Al top contacts. EQEs of >50% in device absorption range comparable to the best reported to date.

Photocurrent vs Morphology

- 3-D topography overlaid with local short-circuit photocurrent measurements of blended P3HT:PCBM film
- Film prepared on top of TCO electrode modified by PEDOT:PSS.
- Darker regions correspond to substantial photocurrent collection.

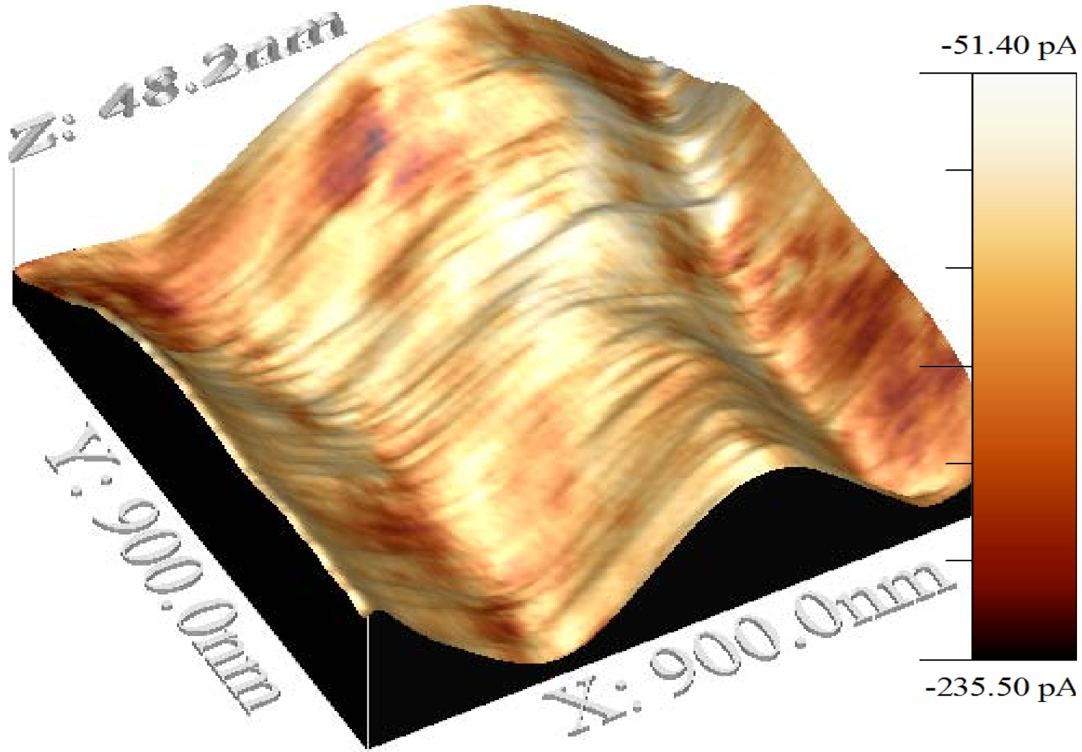

Photocurrent vs Bias Voltage

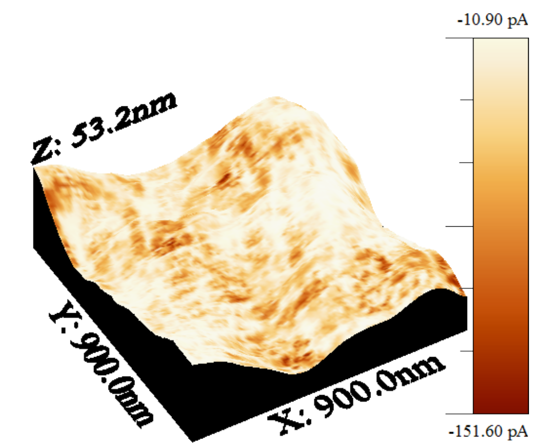

short circuit condition (V = 0 V)

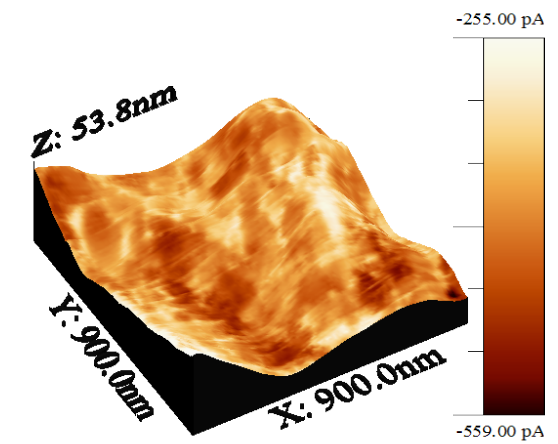

reversed bias(V = -0.3 V)

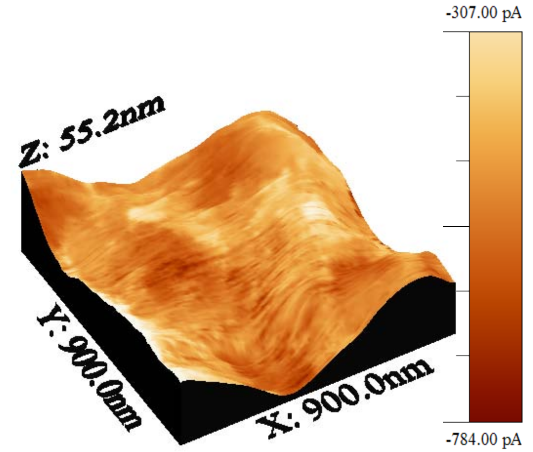

reversed bias(V = -1 V)

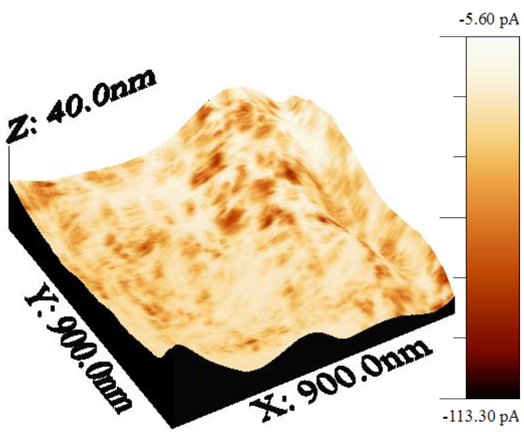

forward bias(V = +0.3 V)

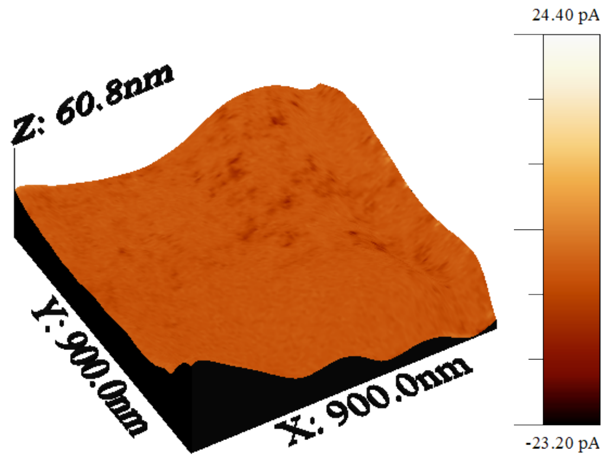

forward bias(V = +0.6 V)

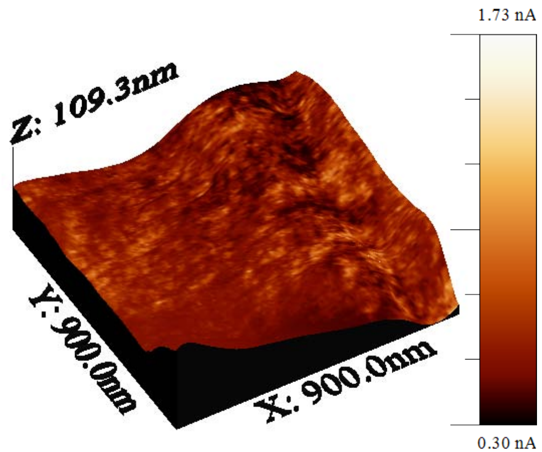

forward bias(V = +1.5 V)

Summary

- Photoconductive SPM is an important tool to study and characterize photovoltaic response of at the nm scale.
- Demonstrated measurements with new results on a well-studied material system
- Continue to add new imaging modalities

Graphene for Post-CMOS Electronics

- CMOS approaching scaling limits
- Graphene more amenable to large-area integration than CNTs
- Measurements of basic materials and device properties needed

NRI

Graphene Production Methods

- Mechanical exfoliation – scotch tape method K.S. Novoselov Proc. Natl. Acad. (2005)
  - Single device process
- Epitaxial graphene on SiC C. Berger et al. J. Phys. Chem. (2004); Science (2006)
  - Wafer scalable process

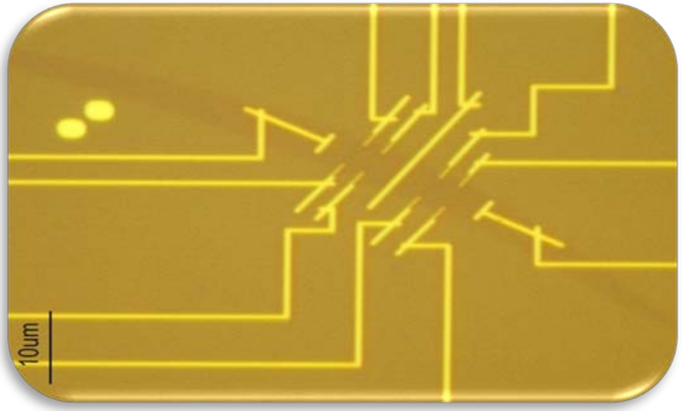

Courtesy of Suyoung Jung, NIST

Courtesy of Walt de Heer, GT

Epitaxial Graphene on C-face SiC

- Multilayers on C-face are electronically decoupled

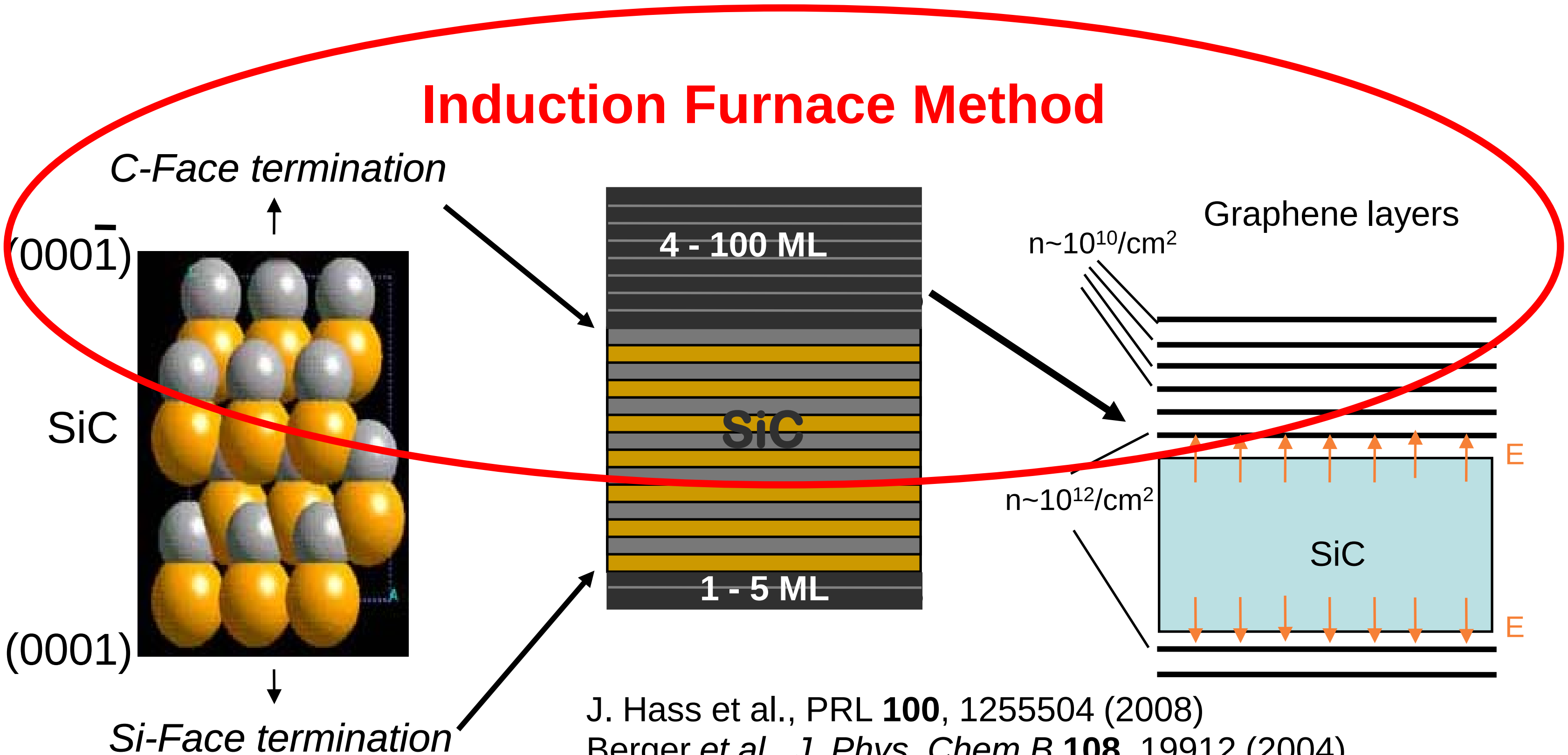

J. Hass et al., PRL **100**, 1255504 (2008)
Berger *et al., J. Phys. Chem B* **108,** 19912 (2004)
Berger *et al., Science* **312,** 1191 (2006)
de Heer *et al., Sol. St. Commun.,* **143**, 92 (2007)

STM Measurement of Quantization

- Direct measurement of density of states with scanning tunneling spectroscopy

Topographic mode

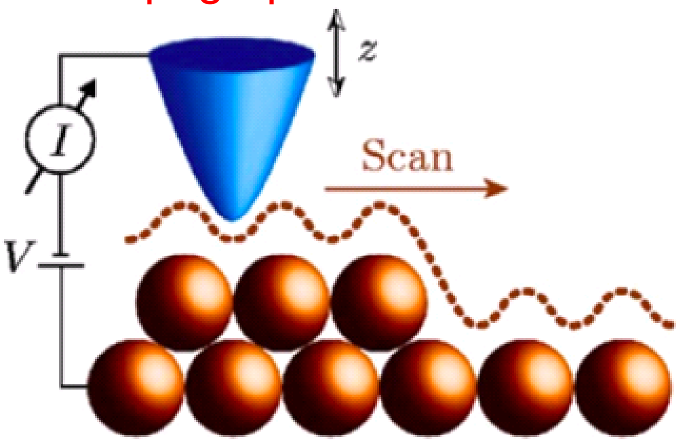

Spectroscopic mode T=4 K

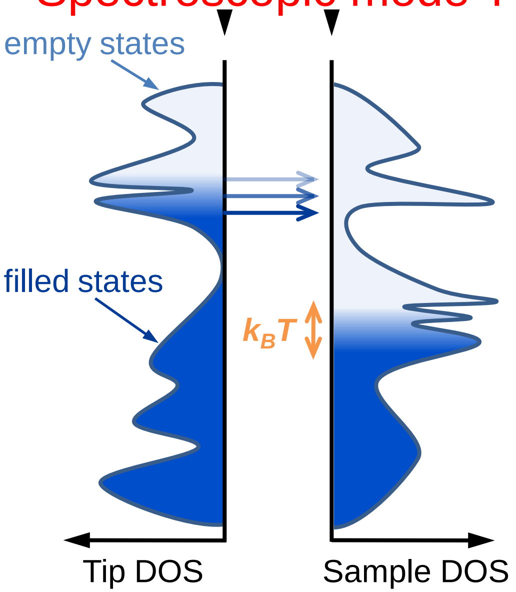

- Spatial LDOS mapping
- Probe the *dI/dV(B,E)* plane

$$dI / dV \propto \mathrm{LDOS}$$

Graphene Magnetic Quantization

- Hallmark of Graphene is the new Landau level quantization and ½ integer QHE – LLs have unequal spacing, special n=0 level

Graphene Landau level spacing

$$\Delta E \approx 1000\ \mathrm{K}@10\ \mathrm{T}$$

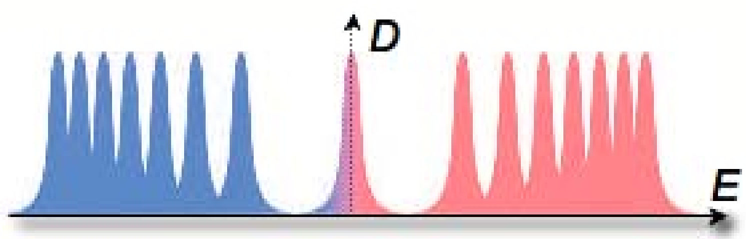

Relativistic:

$$E_n = \mathrm{sgn}(n)\sqrt{2e\hbar\tilde{c}^2\,|n|\,B}$$

“Standard” Landau level spacing

$$\Delta E \approx 10\ \mathrm{K}@10\ \mathrm{T}$$

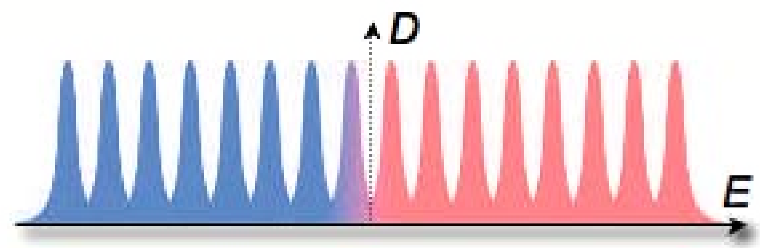

Standard Model:

$$E_n = E_{\pm} \pm \frac{\hbar e}{m^*} B(n+1/2)$$

Graphene Landau Quantization

- Direct measurement of graphene quantization
- Fixing *B*, sweeping *E*

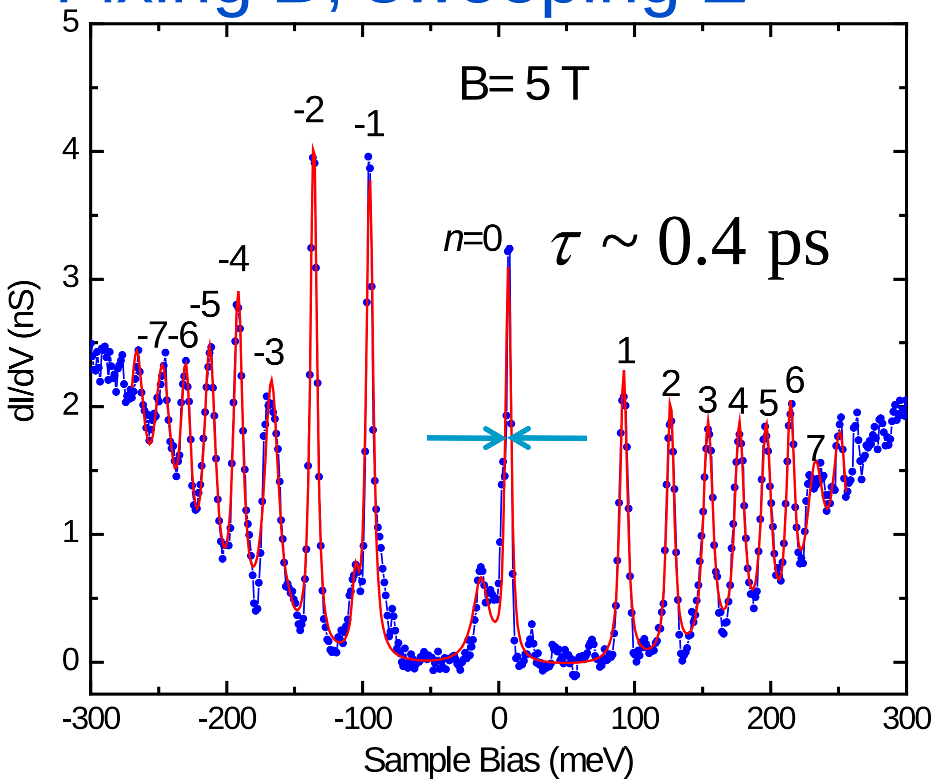

- Quantization obeys graphene scaling
- Full quantization of DOS into Landau levels
- Very sharp LLs
- High mobility

Tunneling Magneto-Conductance Oscillations (TMCO)

- High resolution *E-K* dispersion from TMCO

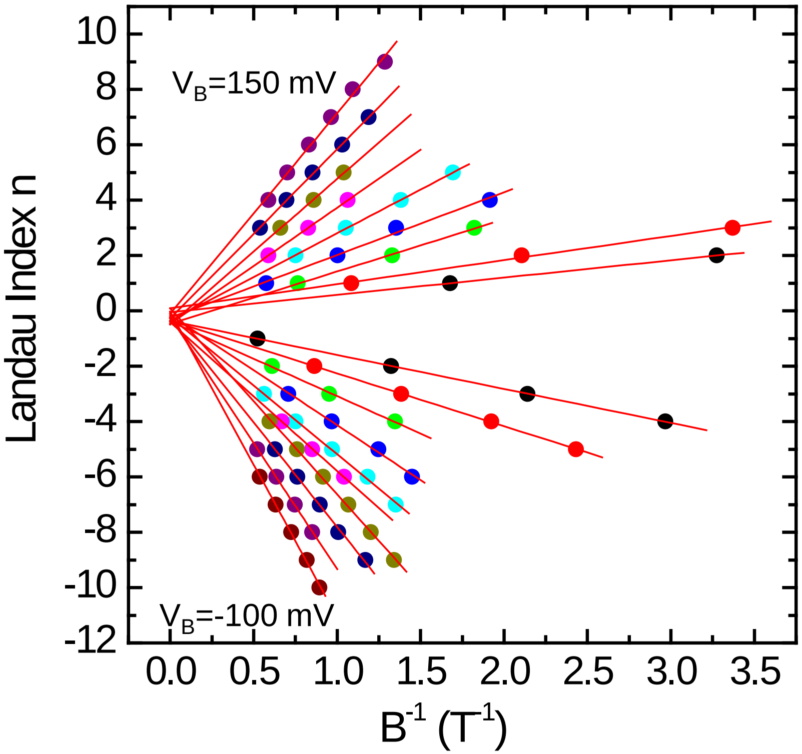

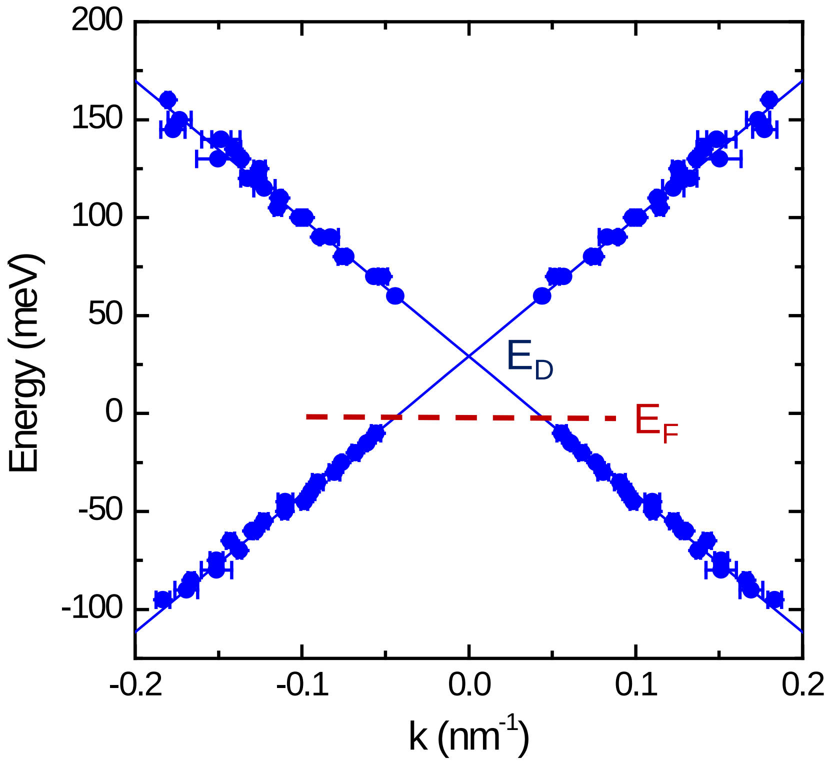

$$\tilde{c} = (1.070 \pm 0.006) \text{ x } 10^6 \text{ ms}^{-1}$$

Origin of Electronic Decoupling

- STM Moiré patterns on c-face epitaxial graphene

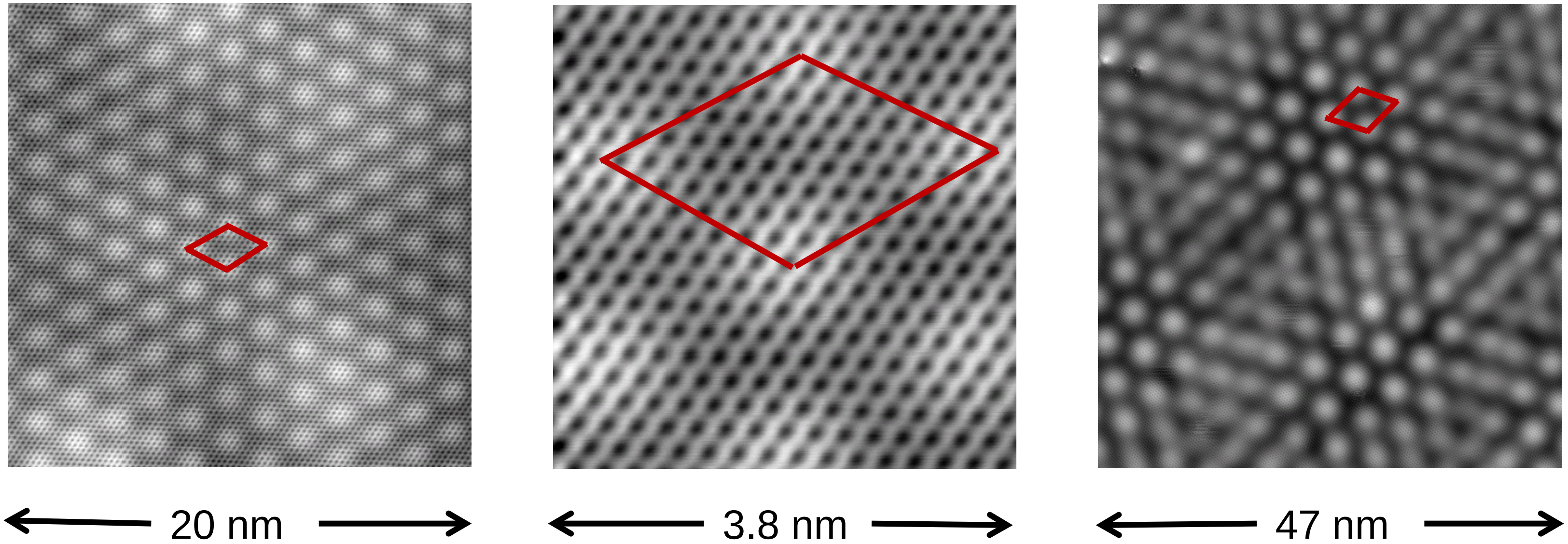

Landau Level Mapping

- Small potential variations in epitaxial graphene

STM

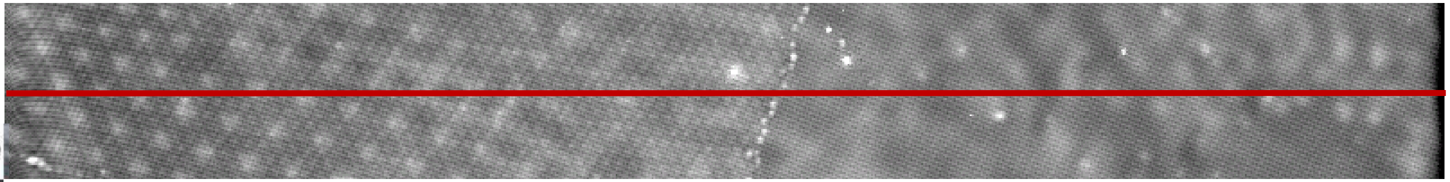

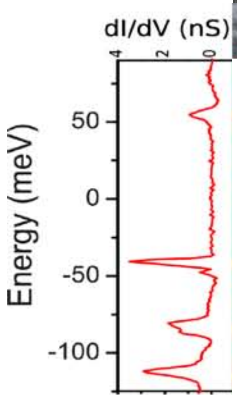

Summary

- Epitaxial graphene on C-face SiC is a good candidate for carbon based electronics
- TMCO is a new STM measurement for high resolution low energy band structure
- Direct measurement of the new graphene quantization with tunneling spectroscopy
- Spatial mapping of LL offers great future potential to understand graphene physics
- See Miller, Kubista, Rutter et al. Science (in press) and www.cnst.nist.gov

Diblocks

NIST

- CNST
  - Alex Liddle
  - Postdoc
    - Gila Stein

Photovolataics

NIST

- CNST
  - Nikolai Zhitenev
  - Postdoc
    - Behrang Hamadani

Graphene

NIST

- CNST
  - Joseph Stroscio
  - Nikolai Zhitenev
  - Mark Stiles
  - Postdocs
    - Gregory Rutter
    - Young Jae Song
    - Sander Otte
    - Suyong Jung
    - Honki Min
  - Visiting Fellow
    - Young Kuk
  - EEEL
    - Dave Newell
    - Curt Richter
    - Mark Keller
- Physics
  - Angie Hight Walker
- MSEL
  - Jan Obrzut
  - Eric Cockayne

Georgia Tech

- Professors
  - Phillip First
  - Walt de Heer
- Students
  - Lee Miller
  - Kevin Kubista
  - Ming Ruan

Univ. Texas Austin

- Professors
  - Allan MacDonald

THANK YOU!

CNST Center for Nanoscale Science & Technology

NIST National Institute of Standards and Technology

Backup Slides

Patterned Media for Hard Disks

Patterned media require:
Feature size < 20 nm
Size control < 2 nm , 3σ
Short-range placement < 2 nm, 3σ
Areas > 10 cm^2

Beyond the limits of top-down nanopatterning

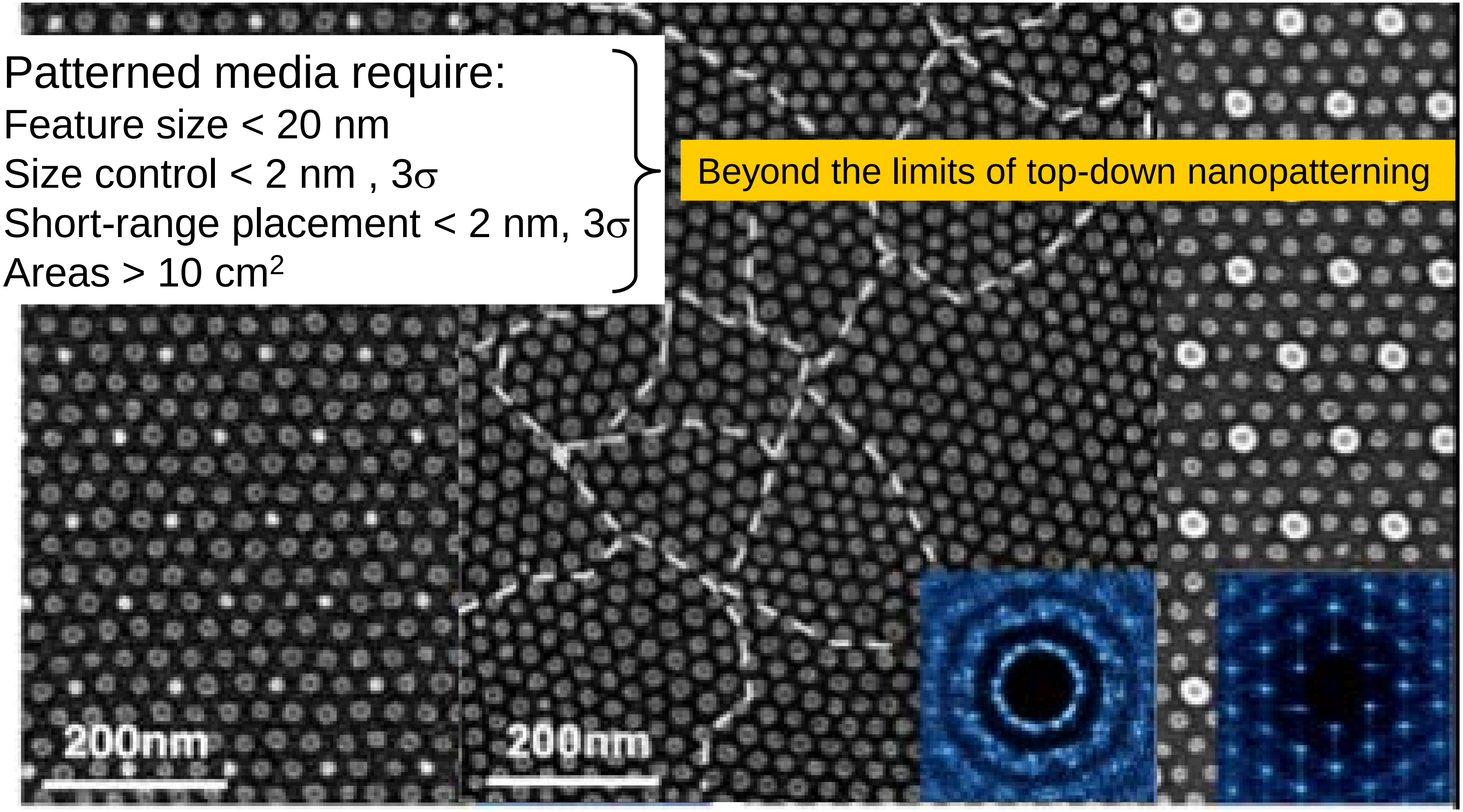

Graphoepitaxy of Self-assembled Block Copolymers on Two Dimensional Periodic Patterned Templates, Ion Bita, Joel K.W. Yang, Yeon Sik Jung, Caroline A. Ross, Edwin L. Thomas, Karl K. Berggren, Science (2008)

Pattern Noise

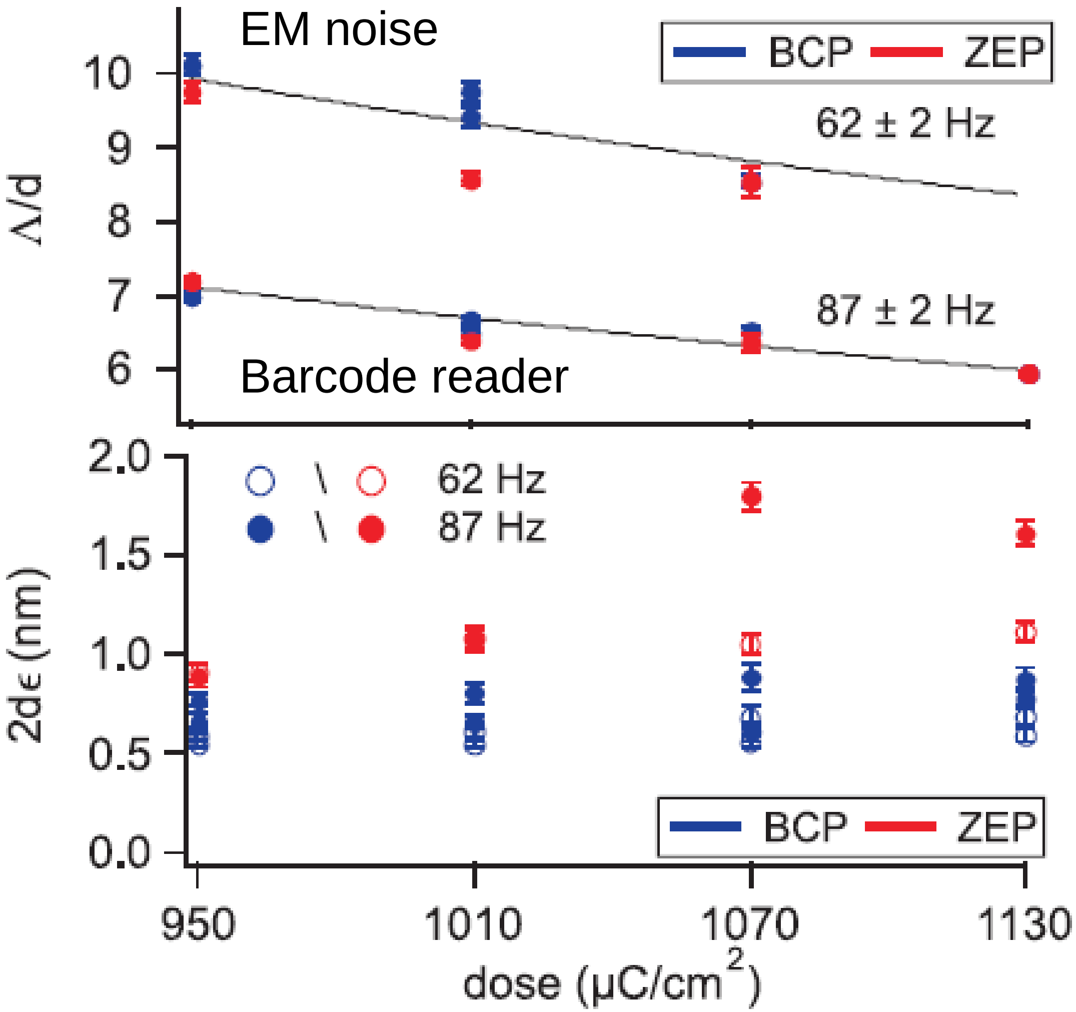

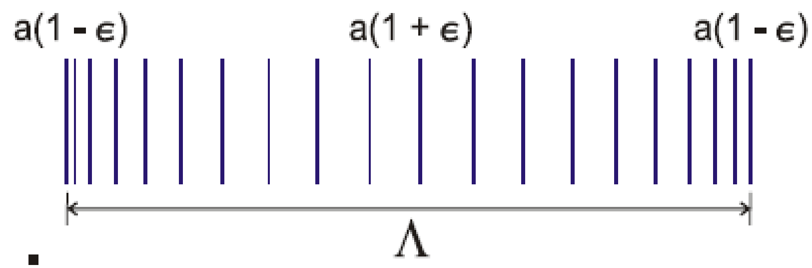

Diffraction picks up subtle variations across large areas

Resist Profiles

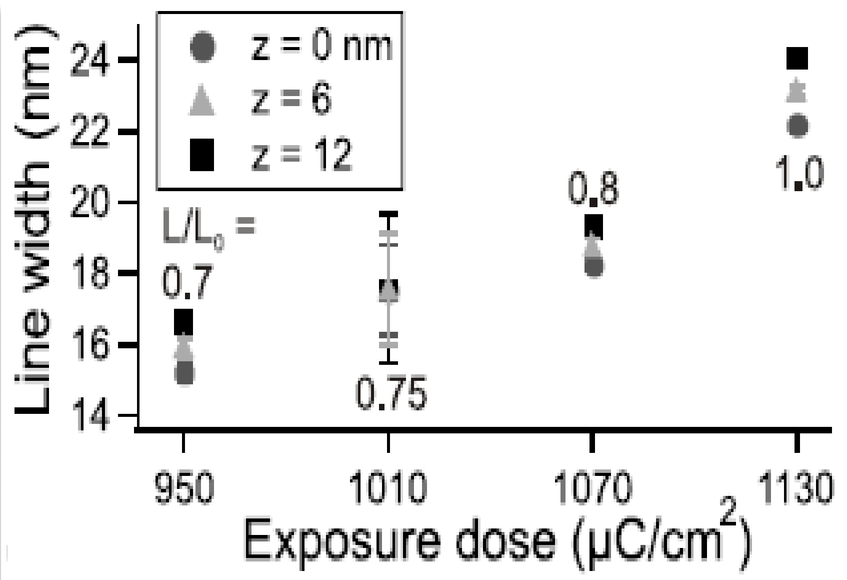

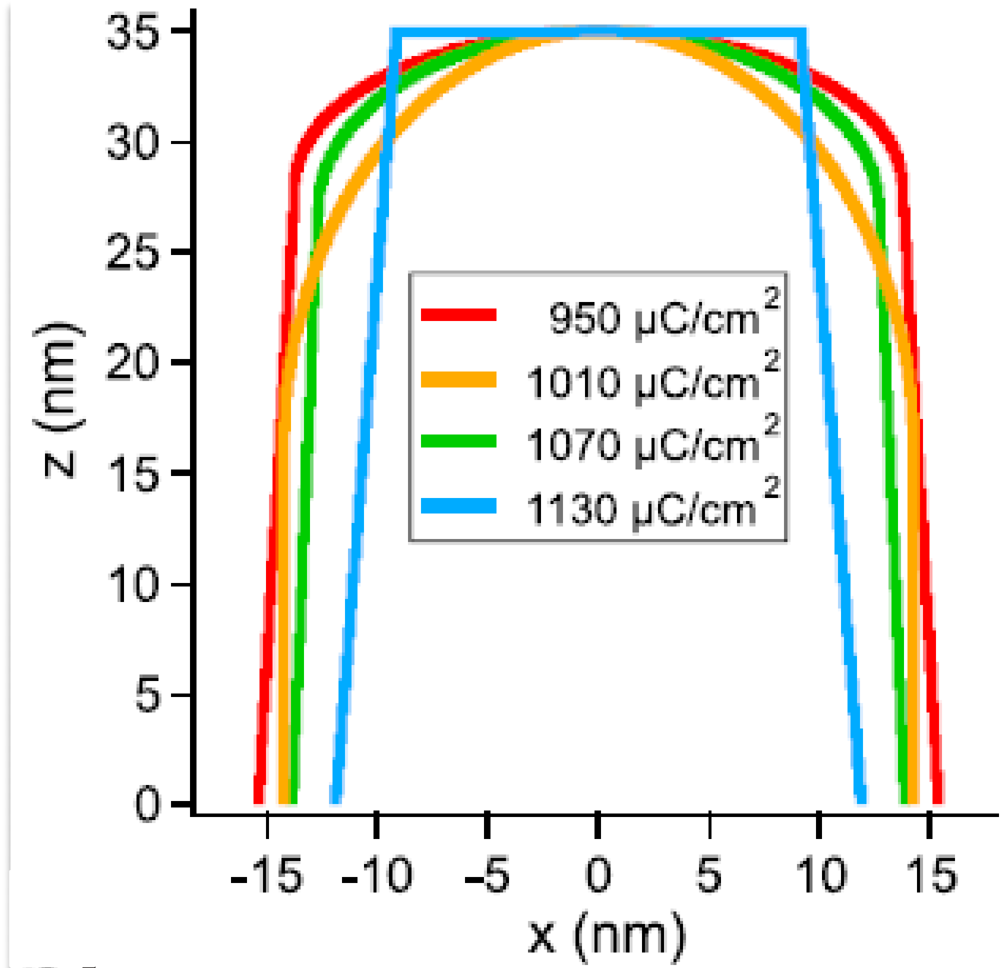

NEXAFS Data

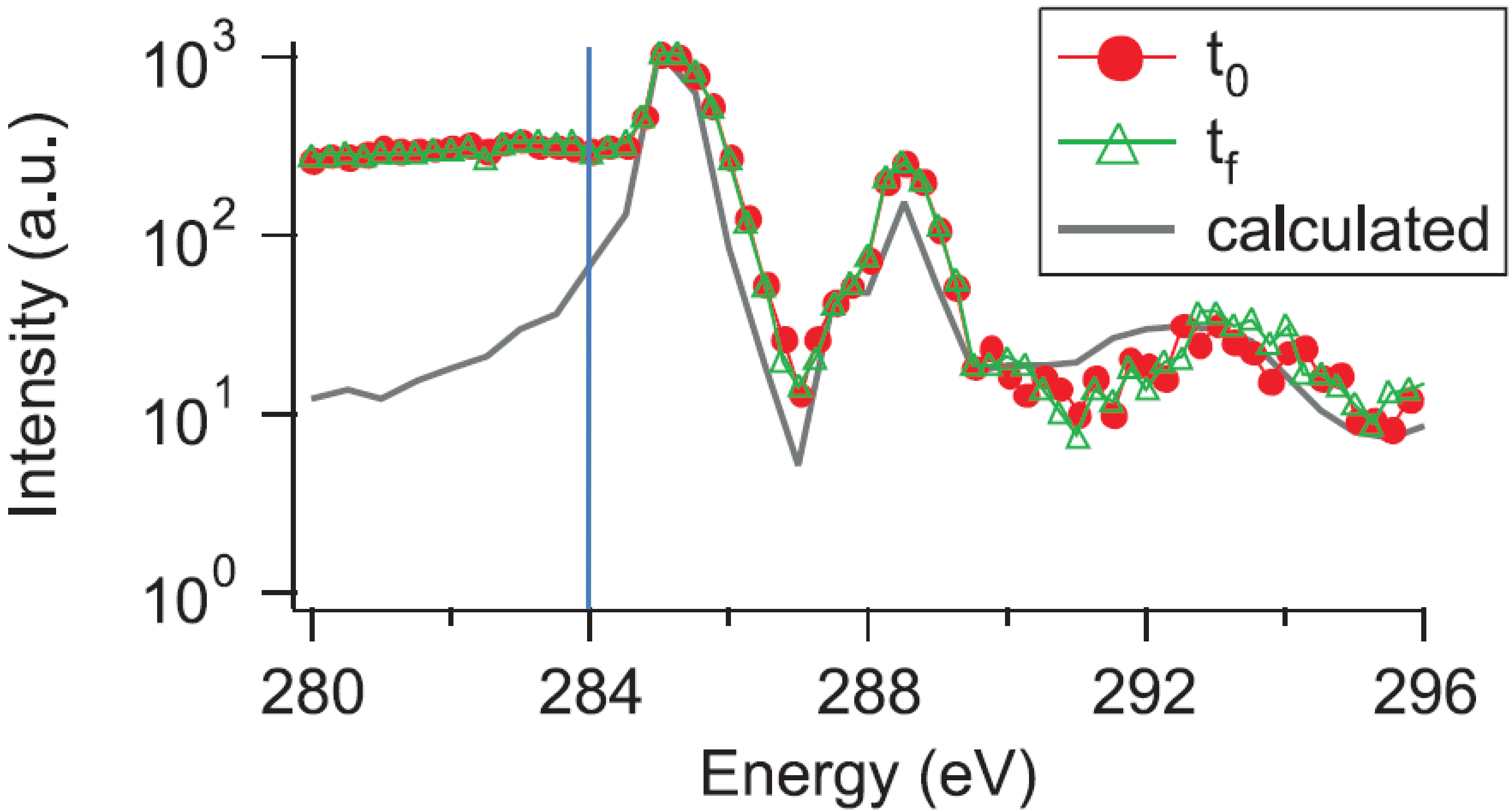

Intensity (a.u.)
10^3
10^2
10^1
10^0
280
284
288
292
296
Energy (eV)
t_0
t_f
calculated

Sidewall Angle

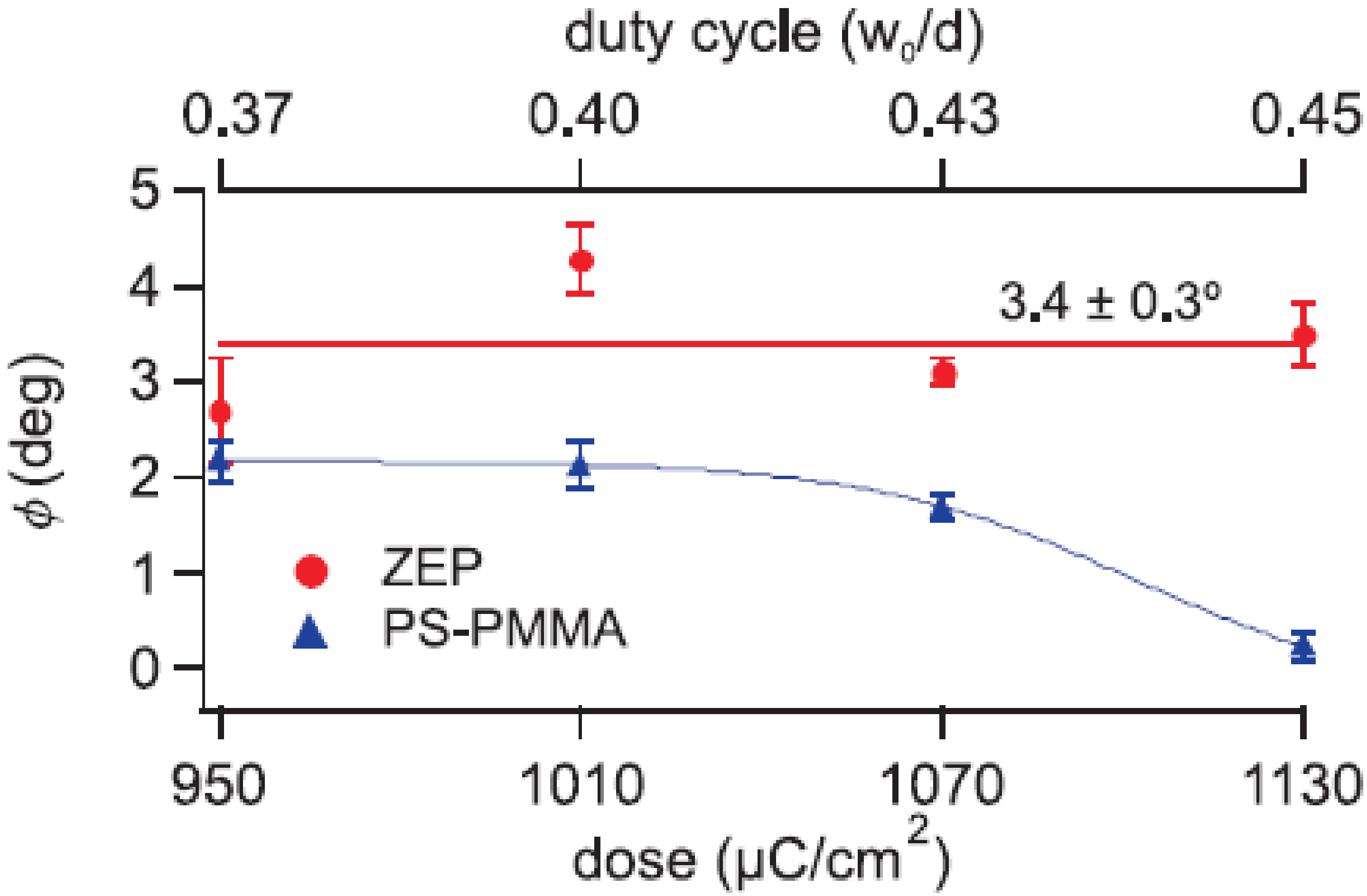

Graphene Production Methods

- Mechanical exfoliation – scotch tape method K.S. Novoselov Proc. Natl. Acad. (2005)

- Epitaxial graphene on SiC C. Berger et al. J. Phys. Chem. (2004); Science (2006)

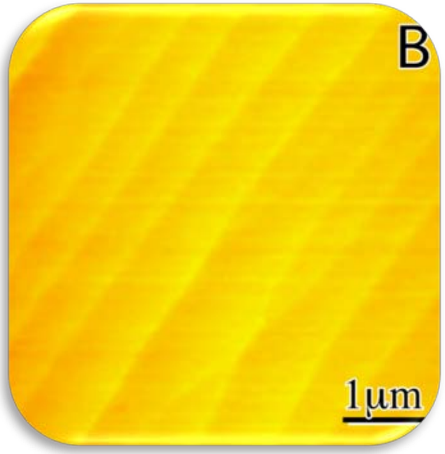

Epitaxial Graphene on SiC

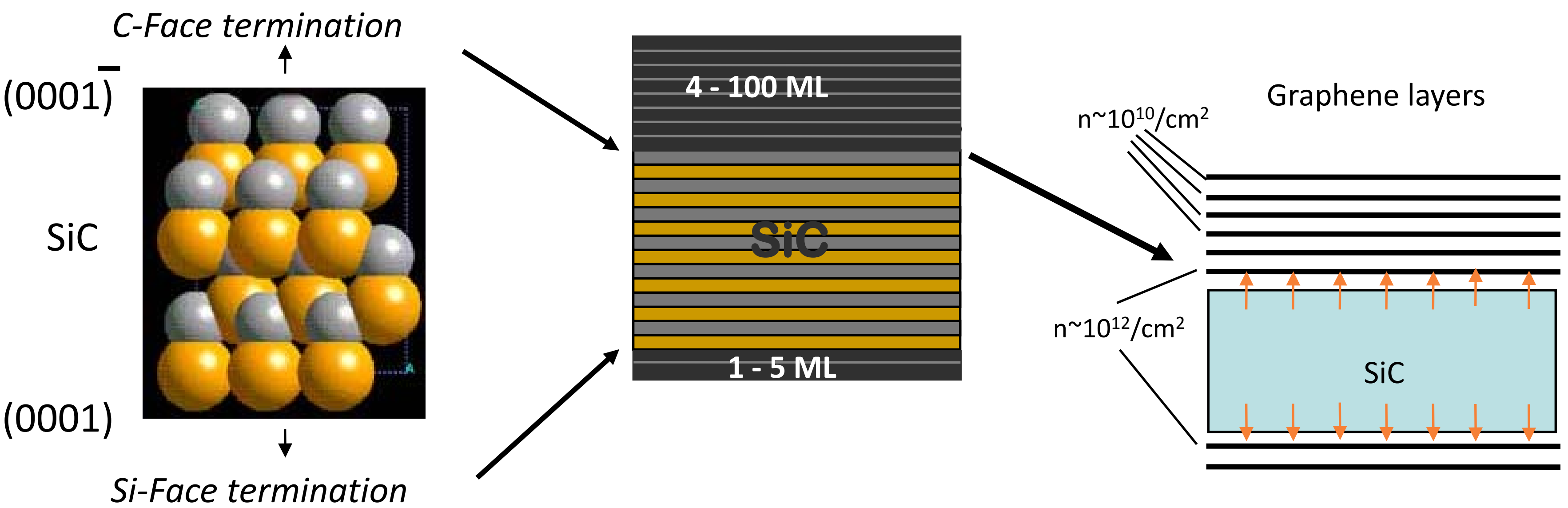

Epitaxial Graphene on Si-face SiC

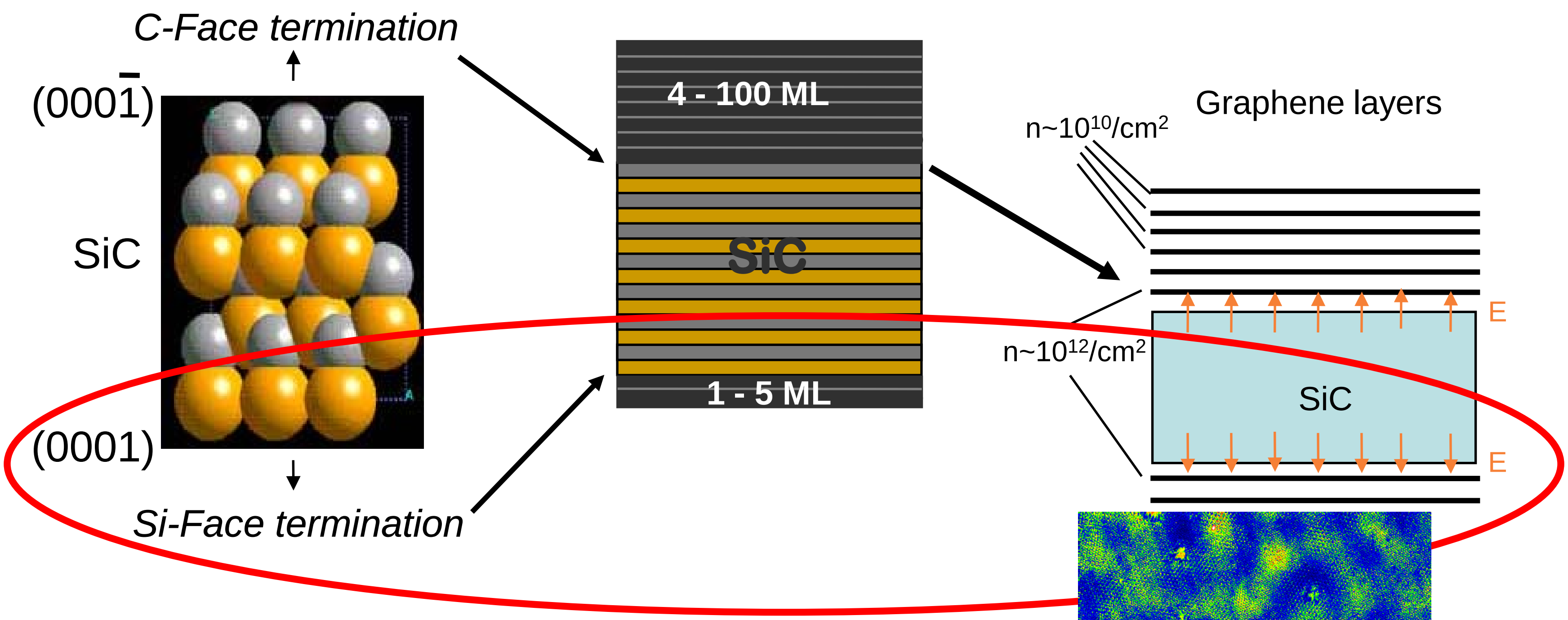

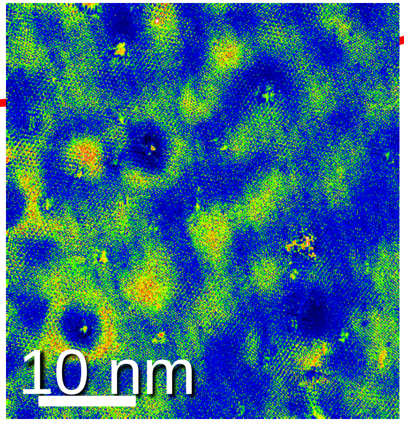

- Our previous work on UHV grown Si-face material
  - AB Bernal stacked epitaxial graphene
  - Intravalley and intervalley scattering; G. Rutter et al. Science (2007); JVST (2008)

Previous STS Measurements on Graphite Surfaces

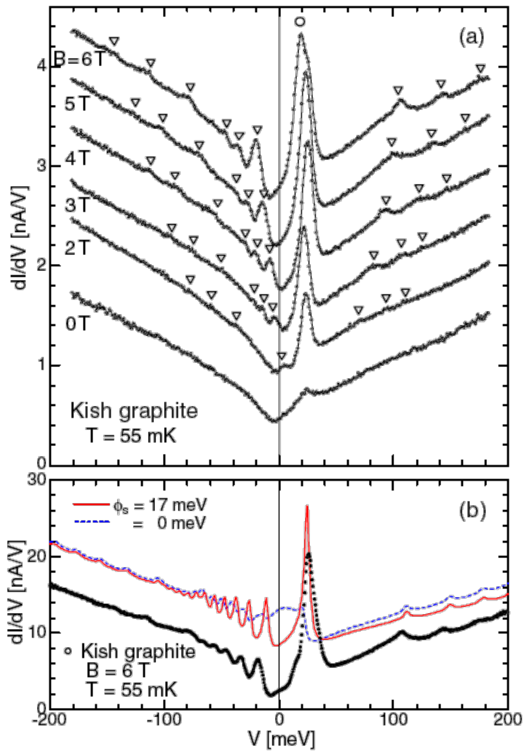

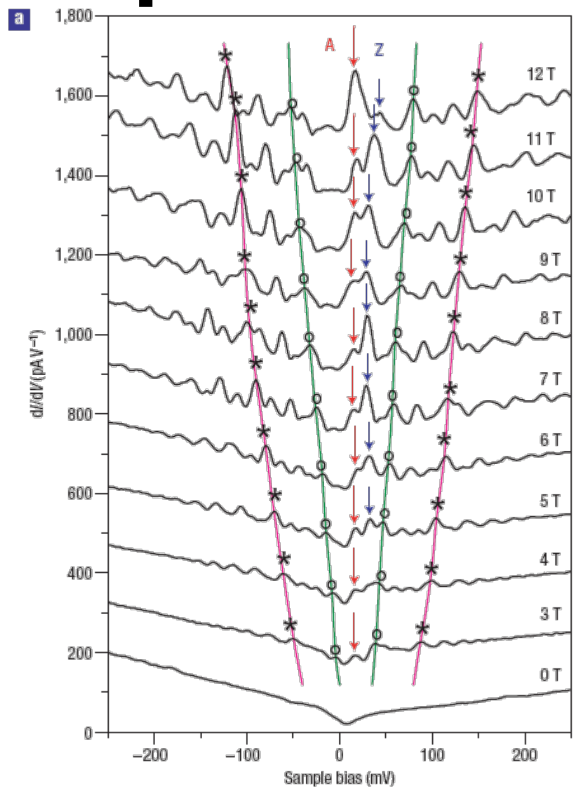

T. Matsui et al. PRL (2005)

G. Li and E. Andrei
Nature Phys. (2007)

- Complex spectra
- Mixture of peaks of linear and non-linear in *B*

Graphene Landau Quantization

- Multilayer epitaxial graphene on SiC is "graphene"! $E_n = \mathrm{sgn}(n)\tilde{c}\sqrt{2e\hbar B|n|}\ , \quad n = \ldots -2,-1,0,1,2,\ldots$

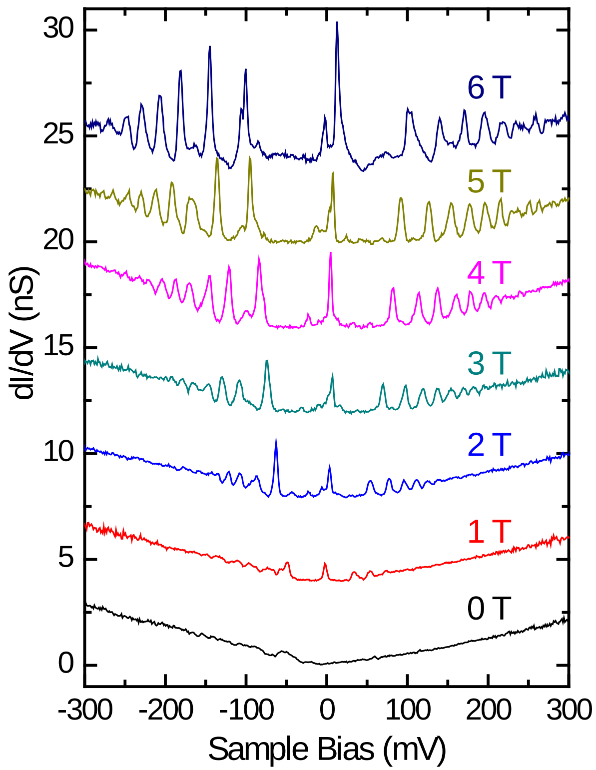

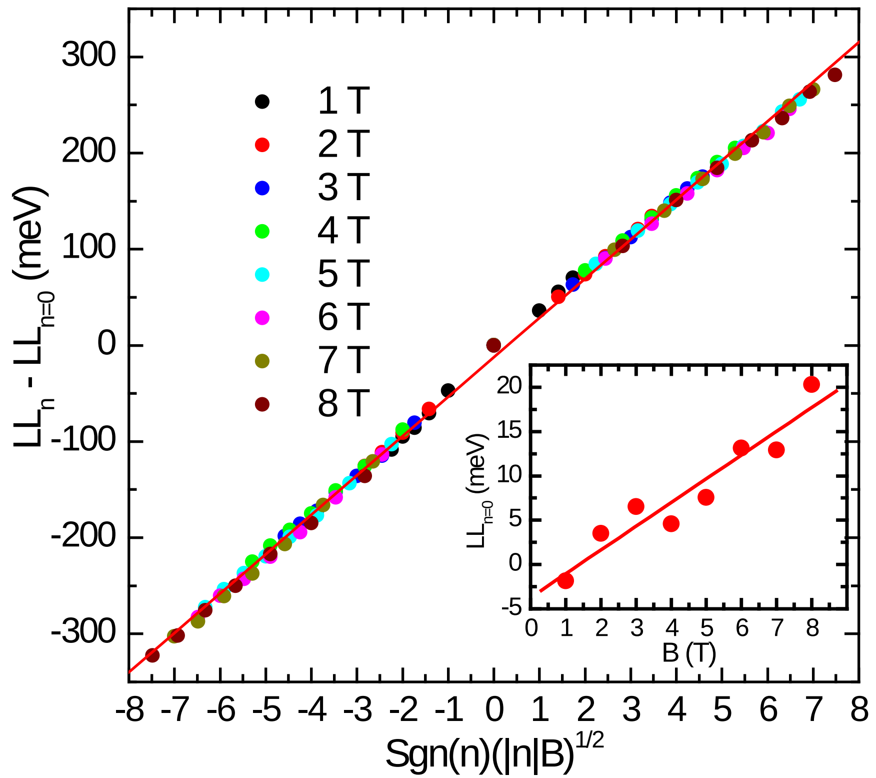

Origin of Electronic Decoupling

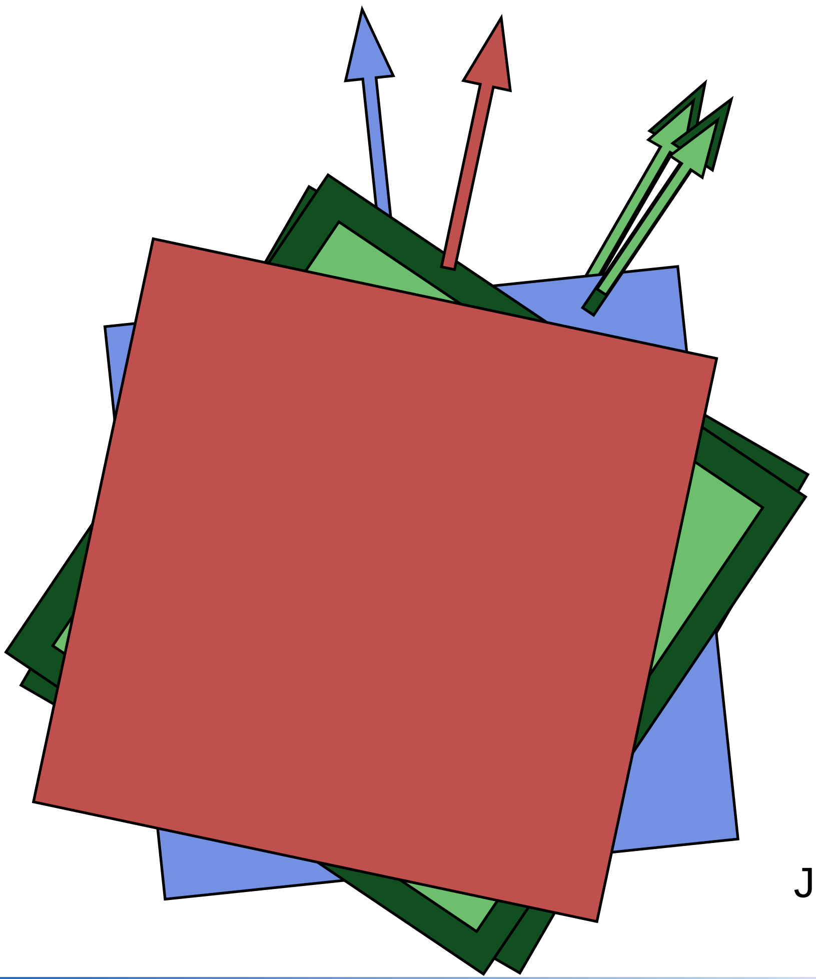

- Layer stacking

Alternating between:
NEAR 30˚ & NEAR 0˚

R7
R31.5C
R31.5
R-3.6
R30C
R30

Joanna Hass et al. PRL **100**, 125504 (2008)

Origin of Electronic Decoupling

- Rotated layers – STM Moiré patterns

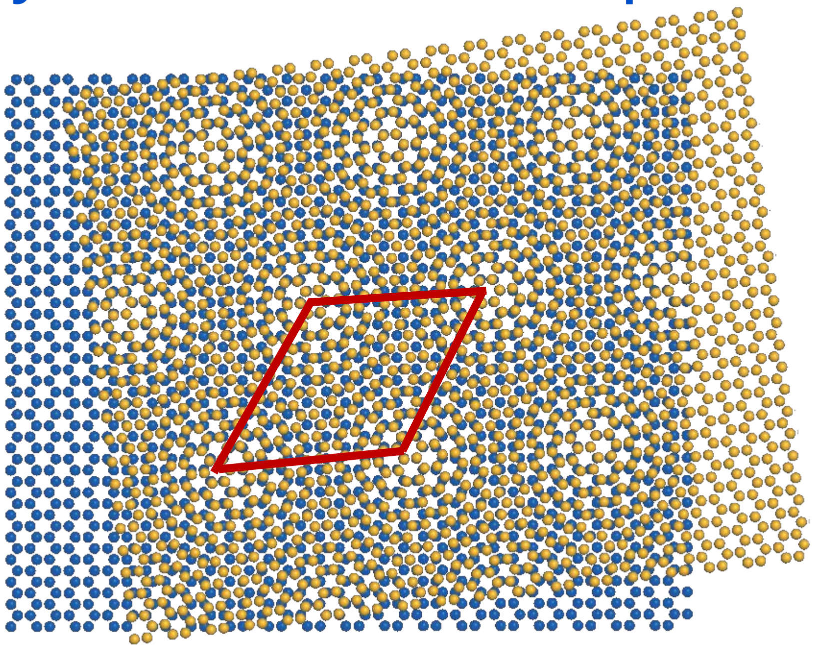

Rotational Domain Boundaries

- Atomically flat and continuous across boundary

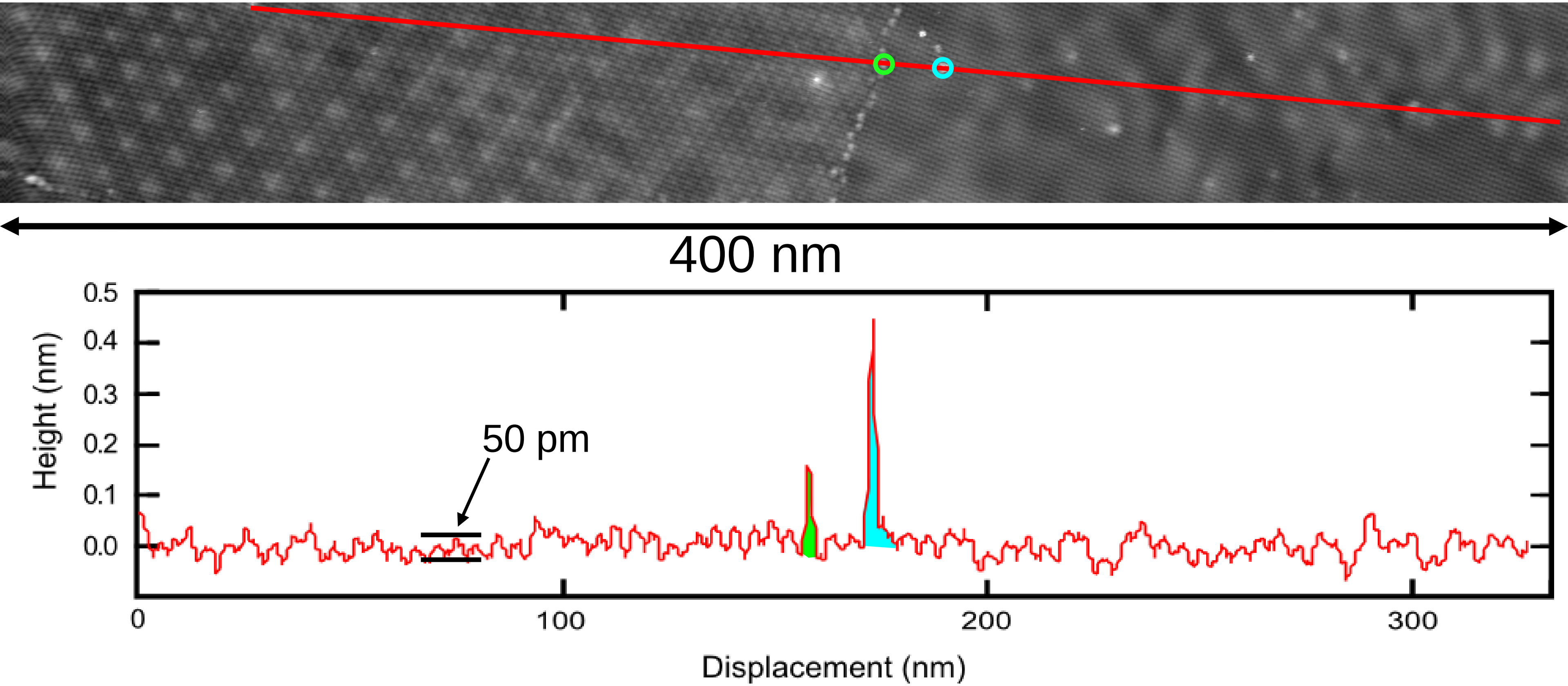

Rotational Domain Boundaries

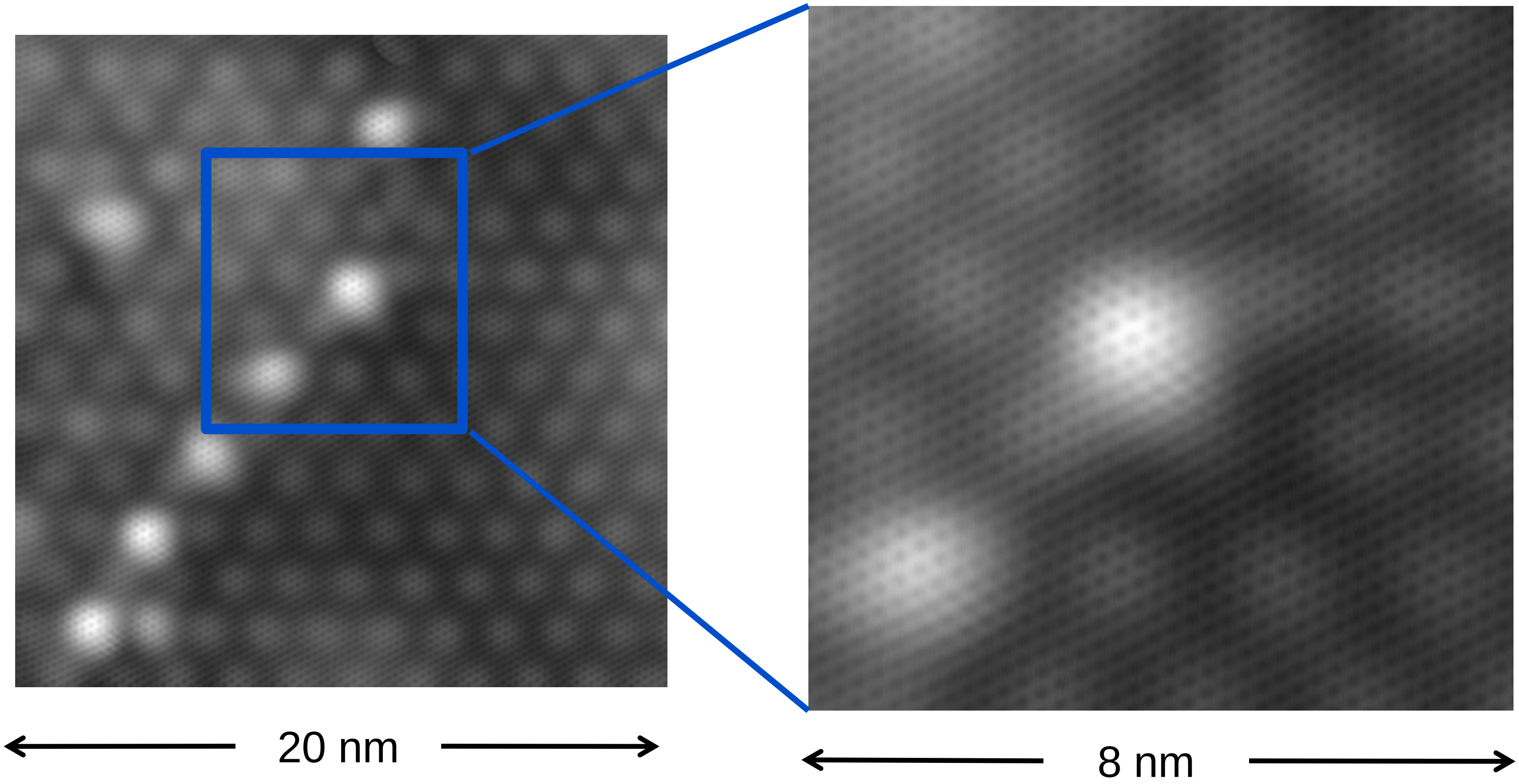

Graphene Landau Quantization

- Complete field scaling of graphene quantization

$$E_n = \mathrm{sgn}(n)\tilde{c}\sqrt{2e\hbar B|n|}\ , \quad n = \ldots -2,-1,0,1,2,\ldots$$

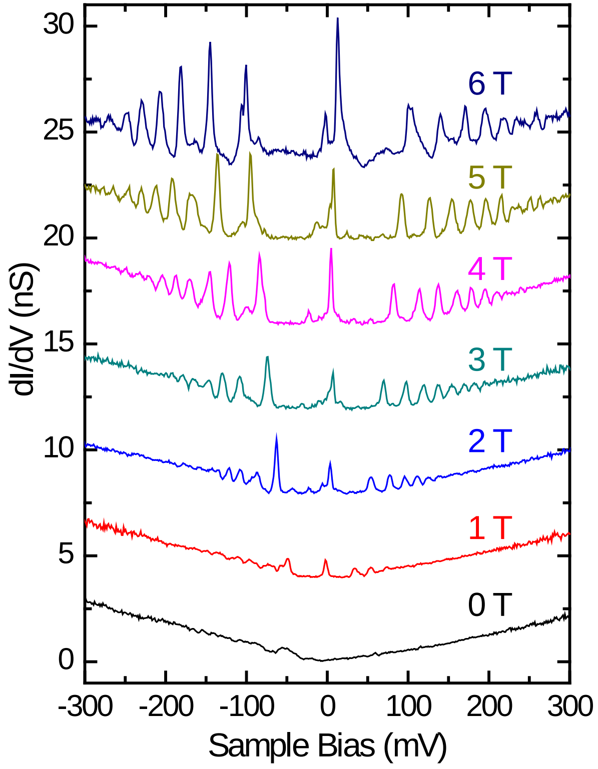

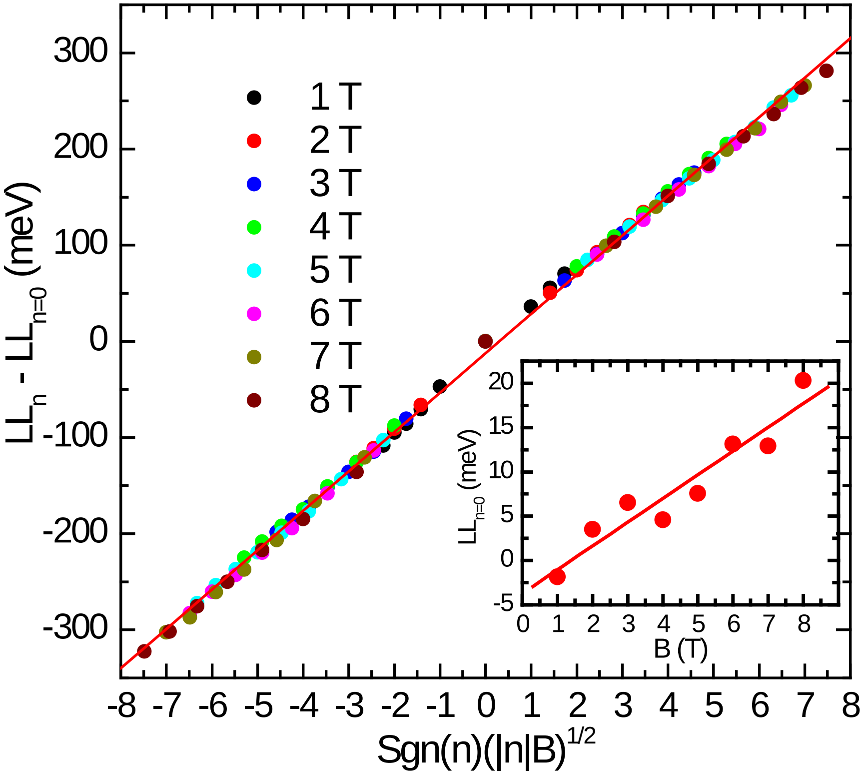

Magnetic Quantization

- Cyclotron motion in a magnetic field
  - Quantized orbits and energy levels

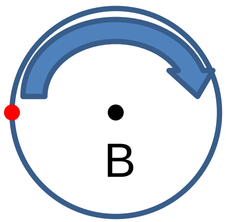

$$E_n = \frac{\hbar e B}{m^*}(n + 1/2) \quad n \geq 0$$ Standard 2DEG

$$E_n = \mathrm{sgn}(n)\sqrt{2e\hbar\tilde{c}^2 |n| B} \quad \mathrm{n{=}0}, \pm 1\ldots$$ Graphene

- Magneto-oscillations
  - De Haas-van Alphen and Shubnikov-de Hass effects; oscillations in physical properties due to quantization of density of states
  - Tunneling magneto-conductance oscillations

Tunneling Magneto-Conductance Oscillations (TMCO)

- Fixing *E* and sweeping *B*

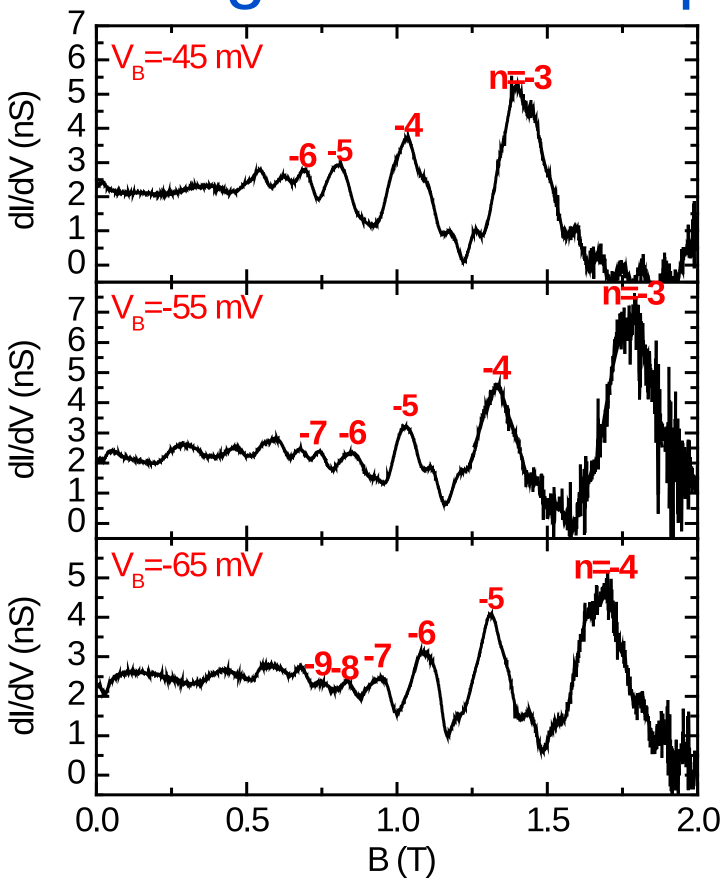

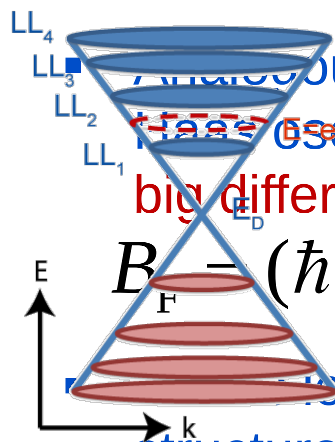

- Analogous to Shubnikov-de Haas oscillations but with one big difference

$$B_F = (\hbar / 2\pi e) A_F \qquad A_F \to A_E$$

- Allows low energy band structure to be measured with high energy and momentum resolution

Origin of Electronic Decoupling

- Rotated layers with Preferred Domains- LEED

SiC bulk

Graphene

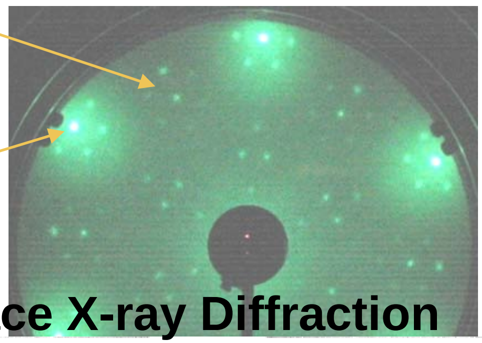

Surface X-ray Diffraction

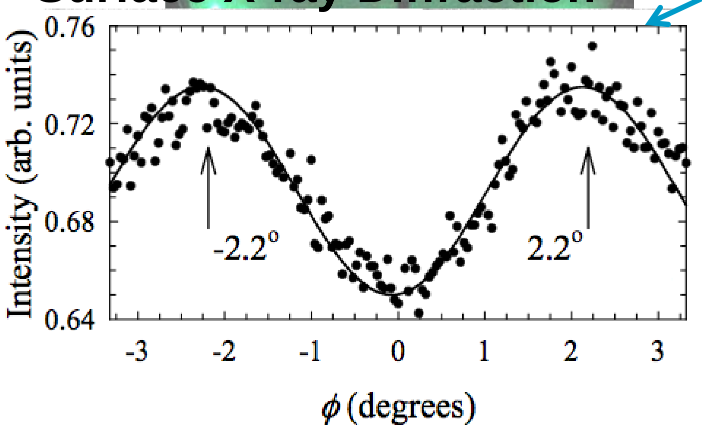

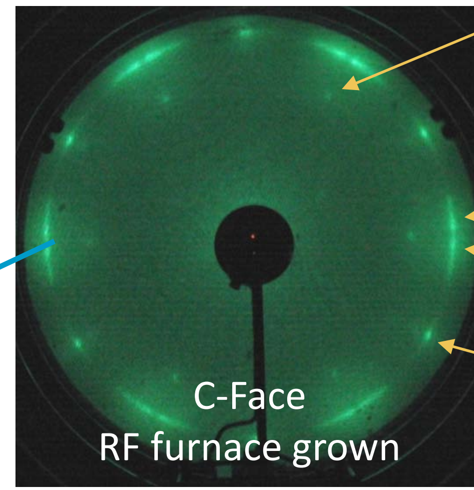

72.2eV

Graphene
R±2.2

Graphene
R30

Joanna Hass et al. PRL **100**, 125504 (2008)

Origin of Electronic Decoupling

- Rotated bilayer maintains linear dispersion

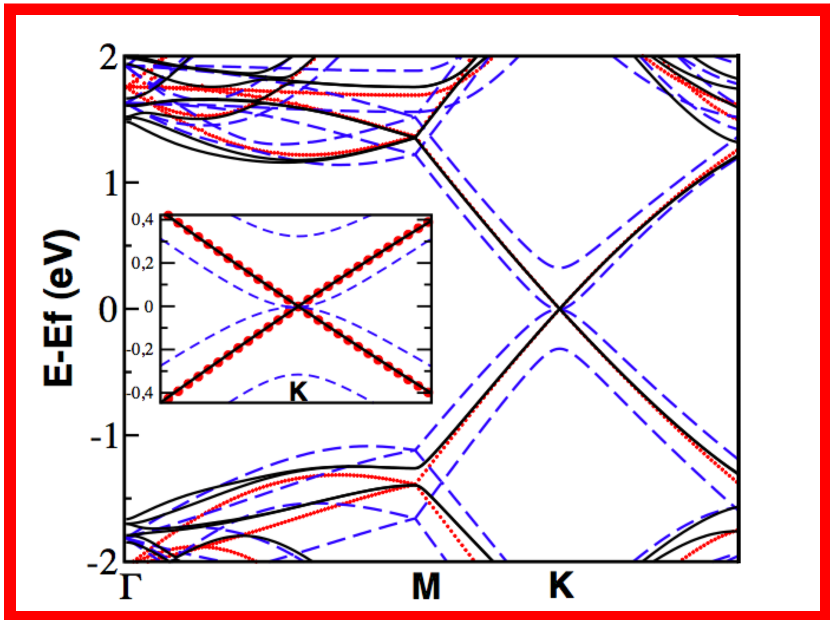

R30/R2 fault pair
Graphene bilayer
Isolated graphene sheet

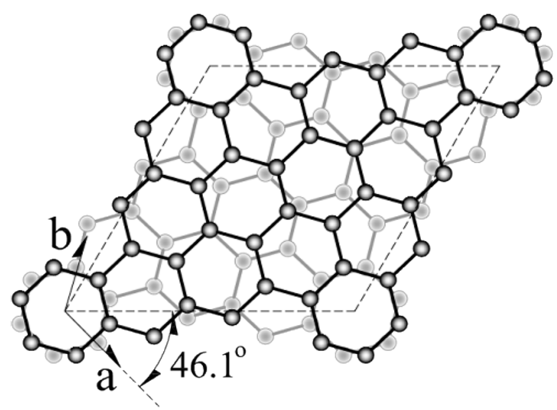

F. Varchon and L. Magaud, CNRS

Tunneling Magneto-Conductance Oscillations (TMCO)

- Fan plot; Landau index *n* vs. 1/*B*

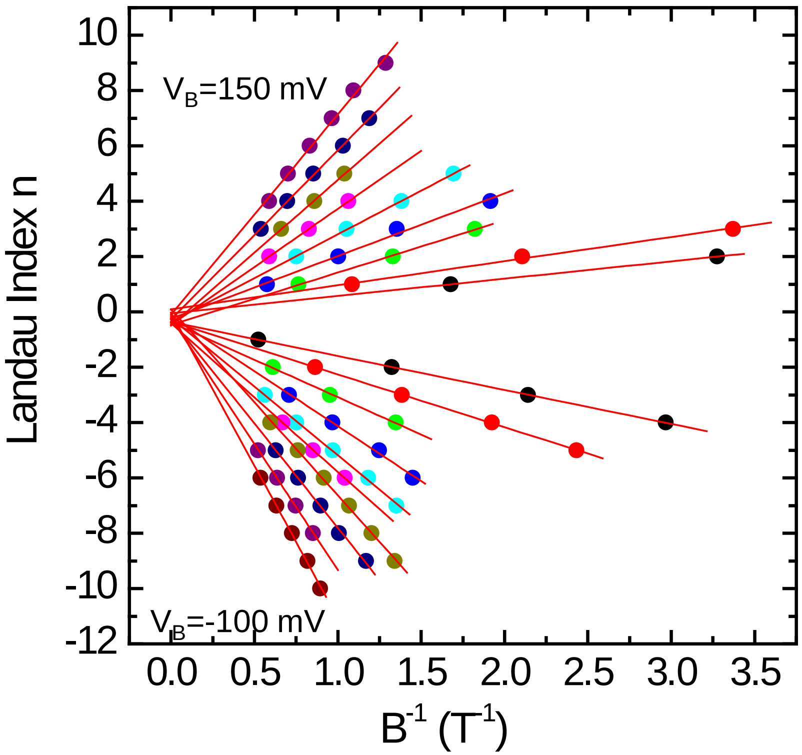

Slope of *n* vs. *1/B* determines B_E

$$B_E = (\hbar / 2\pi e) A_E$$

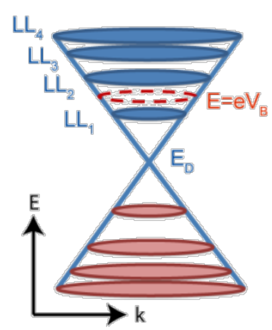

Circular energy contours at $E=V_B$

$$A_E = \pi k_E^2$$

$$k_E = \left((4\pi e / h) B_E \right)^{1/2}$$